Projections from Bed Nuclei of the Stria Terminalis, Anteromedial Area: Cerebral Hemisphere Integration of Neuroendocrine, Autonomic, and Behavioral Aspects of Energy Balance

HONG-WEI DONG and **LARRY W. SWANSON**[*]

Department of Biological Sciences, University of Southern California, Los Angeles, California 90089-2520, USA

Abstract

The anteromedial area of the bed nuclei of the stria terminalis (BSTam) is the relatively undifferentiated region of the anterior medial (anteromedial) group of the bed nuclei of the stria terminalis (BSTamg), which also includes the more distinct dorsomedial, magnocellular, and ventral nuclei. The overall pattern of axonal projections from the rat BSTam was analyzed with the PHAL anterograde pathway tracing method. Brain areas receiving relatively moderate to strong inputs from the BSTam fall into five general categories: *neuroendocrine system* (regions containing pools of magnocellular oxytocin neurons, and parvicellular corticotropin-releasing hormone, thyrotropin-releasing hormone, somatostatin, and dopamine neurons); *central autonomic control network* (central amygdalar nucleus, descending paraventricular nucleus, and ventrolateral periaqueductal gray); *hypothalamic visceromotor pattern generator network* (5 of 6 known components); *behavior control column* (descending paraventricular nucleus and associated arcuate nucleus; ventral tegmental area and associated nucleus accumbens and substantia innominata); and *behavioral state control* (supramammillary and tuberomammillary nuclei). The BSTam projects lightly to *thalamocortical feedback loops* (via the medial-midline-intralaminar thalamus). Its pattern of axonal projections, combined with its pattern of neural inputs (the most varied of all BST cell groups), suggest that the BSTam is part of a striatopallidal differentiation involved in coordinating neuroendocrine, autonomic, and behavioral or somatic responses associated with maintaining energy balance homeostasis.

Indexing terms

amygdala; autonomic; arcuate nucleus; bed nucleus of the stria terminalis; eating; hypothalamus; neuroendocrine; paraventricular nucleus

INTRODUCTION

This is the last in a series of eight reports (Dong et al., 2000, 2001b; Dong and Swanson, 2003, 2004a,b; 2005a,b) on the structural distribution of axonal projections from the various cellular differentiations associated with the bed nuclei of the stria terminalis (BST), a non-laminated region of the cerebral hemisphere that develops from the medial or pallidal

[*]Correspondence to: Dr. L.W. Swanson, Hedco Neuroscience Building, 3641 Watt Way, University of Southern California, Los Angeles, California 90089-2520. Voice: (213)740-5892/Fax: (213)741-0561. Email: lswanson@usc.edu.
Dr. Dong's present address is Allen Institute for Brain Science, 551 N 34th Street, Suite 200, Seattle, WA 98103.
Associate Editor: Paul Sawchenko

ventricular ridge (Bayer, 1987; Ju and Swanson, 1989; Ju et al., 1989; Alvarez-Bolado and Swanson, 1996) and receives a massive, topographically organized input from the amygdalar region of the temporal lobe (Johnston, 1923; de Olmos and Ingram, 1972; Krettek and Price, 1978; Dong et al., 2001a). Here we focus on the anteromedial area (BSTam), the relatively undifferentiated region of the anterior medial (anteromedial) group (BSTamg), which also includes the more distinct dorsomedial nucleus (Dong and Swanson, 2005a) and the magnocellular and ventral nuclei (Dong and Swanson, 2005b). The overall organization of BSTam projections has not been examined previously.

MATERIALS AND METHODS

They were identical to those described earlier (Dong and Swanson, 2003). Experiments were performed according to *NIH Guidelines for the Care and Use of Laboratory Animals*, and all protocols were approved by the University of Southern California Institutional Animal Care and Use Committee. The experiments described here were chosen from a collection of over 200 PHAL injections in all parts of the BST. Adult male Harlan Sprague-Dawley rats (300–350 g) received a single, stereotaxically placed iontophoretic injection of a 2.5% solution of PHAL (Vector Laboratories, Burlingame, CA), prepared in 0.1 M sodium phosphate-buffered saline (NaPBS), pH 7.4, into various regions of the BST through a glass micropipette (15 μm tip diameter) by applying a positive current (5 μA, 7 sec on/off intervals) for 7–10 min. Animals were anesthetized for stereotaxic surgery with an equal mixture of ketamine and xylazine solutions (50 mg/ml ketamine, 10 mg xylazine/ml; 1 ml/ kg body weight).

After surviving 14–16 days, the rats were deeply anesthetized with pentobarbital (40 mg/kg body weight, intraperitoneal) and perfused transcardially with 150 ml of 0.9% NaCl followed by 300 ml of ice-cold 4% paraformaldehyde in 0.1 M borate buffer (pH 9.5). Brains were removed, post-fixed overnight at 4°C in the same fixative containing 10% sucrose, and frozen. Then serial 30 μm-thick sections (1-in-4) were cut in the transverse plane on a sliding microtome. One complete series of sections was processed to detect PHAL using the immunohistochemical procedure described elsewhere (Gerfen and Sawchenko, 1984; Petrovich and Swanson, 1997). PHAL-containing cells (in the injection sites) and fibers were plotted with the aid of a camera lucida onto cytoarchitectonic drawings of adjacent thionin-stained sections, and then transferred onto a series of standard drawings of the rat brain (Swanson, 2004) with the aid of a computer (Apple, Mac PowerPC G4, Adobe Illustrator CS). Photomicrographs were taken with a CCD camera (Diagnostics Instruments, Sterling Heights, MI) or with a Wild Leitz 35 mm camera mounted on a Wild M3Z stereozoom microscope. Film was digitized with a Nikon scanner (LS-1000), and all digital files were composed, and adjusted for brightness and contrast, in Adobe Photoshop 5 using a Mac PowerPC G4. Parceling of the rat brain, the terminology for describing morphological features of PHAL-labeled axons, and mapping strategies and procedures follow Swanson (2004), unless indicated otherwise.

RESULTS

Nomenclature

The BST parcellation used here derives from the cyto- and chemoarchitectonic work of Ju and colleagues in the rat (Ju and Swanson, 1989; Ju et al., 1989). However, minor changes based on later connectional and cytoarchitectonic analyses have been made to boundaries and the nomenclature hierarchy (see Dong et al., 2001a; Swanson, 2004). For example, when reexamining the BST anterolateral area, it became clear that undifferentiated regions dorsal and ventral to the anterior commissure share similar connections and cellular architecture, so that the original anterolateral area (dorsally) and subcommissural zone

(ventrally) were combined into a newly defined, larger anterolateral area (Dong and Swanson, 2004a). Subsequent experience with the BSTamg has led to similar conclusions, although the undifferentiated region of the BSTam is more complex than the BST anterolateral area.

Based on the work of Ju and colleagues (Ju and Swanson, 1989; Ju et al., 1989), Dong and Swanson (2001a) defined two divisions of the BSTamg: the anterodorsal area (with rostral and caudal ends and a central condensation), and the anteroventral area—with an undifferentiated region (also called the anteroventral area) and four embedded nuclei (dorsomedial, dorsolateral, ventral, and magnocellular). The ambiguity created by using the term anteroventral area for the division and for the undifferentiated region within it can be solved in the traditional way by referring to the latter (undifferentiated region) as the anteroventral region proper.

In their original description, Ju and colleagues (Ju and Swanson, 1989; Ju et al., 1989) pointed out that BST anterior division regions immediately dorsal and ventral to the anterior commissure (the anterodorsal area, dorsolateral nucleus, and anteroventral area proper) display rather similar chemo- and cytoarchitectonic features, and it was shown later that amygdalar projections to all three regions are also similar (Dong et al., 2001a). Experiments analyzed for this and the accompanying papers (Dong and Swanson, 2005a,b) indicate that projection patterns from the bulk of all three regions are essentially identical as well. Considering this evidence together, we here simplify BST parcellation and nomenclature by combining into a single entity—the *BST anteromedial area* (BSTam)—the following components: a) the anterodorsal area, b) the anteroventral area proper of Ju and colleagues (Ju and Swanson, 1989; Ju et al., 1989), c) the rostral third of the dorsolateral nucleus (Atlas Level 20; Swanson, 1998–1999), d) the rostral tongue of the BST dorsomedial nucleus (Atlas Levels 16–19; Swanson, 1998–1999; also see Dong and Swanson, 2005a), and e) the lateral two-thirds of the ventral nucleus on Atlas Level 21 of Swanson (1998–1999; also see Dong and Swanson, 2005b). In their original description Ju and colleagues noted a central condensation (BSTcc) in the anterodorsal area. While this slight increase in cell packing density can be observed, connections associated with this region (Dong et al., 2001a, and present observations) are similar to those from the rest of the anterodorsal area (and BSTam as a whole), so to simplify even further, this differentiation is no longer routinely identified in drawings and photographs of the BST.

The redefined borders of the BSTam enclose a region with essentially the same cytoarchitectonic and chemoarchitectonic features described for the original BSTam (Ju and Swanson, 1989; Ju et al., 1989). The most characteristic feature is a relatively high density of the predominant cell type in Nissl-stained sections: small, round to oval neurons. There are also moderate numbers of corticotropin-releasing hormone-immunoreactive and neurotensin-immunoreactive neurons and fibers in the BSTam, along with moderate numbers of substance P-immunoreactive and cholecystokinin-immunoreactive fibers.

At the same time, this cytoarchitectonic and connectional evidence suggests that two small regions of the anterodorsal area should be reassigned such that the ventral tail of the anterodorsal area (as identified in Swanson 1998–1999, Atlas level 19) is part of the anterolateral area, and the caudal tip of the anterodorsal area (as identified in Swanson 1998–1999, Atlas level 20) becomes the rostral pole of the BST principal nucleus.

Although these considerations obviously are detailed, they nevertheless do lead to considerable simplification of BSTamg parceling and nomenclature by eliminating the original anterodorsal area with its three differentiations, anteroventral area, and dorsolateral nucleus; and by recognizing a compact, well-defined dorsomedial nucleus (just on Atlas

Levels 20 and 21, rather than Atlas Levels 16–20, of Swanson 1998–1999), a reassignment that is further considered in Dong and Swanson (2005a). The revised and simplified parceling scheme just discussed is adopted in Swanson (2004). For descriptive purposes, regions of the BSTam dorsal to the anterior commissure may be referred to as the dorsal BSTam (BSTamd), whereas regions of the BSTam ventral to the anterior commissure may be referred to as the ventral BSTam (BSTamv).

Injection sites

A total of 18 experiments were analyzed to determine the overall projection pattern of the BSTam (Figs. 1–3). Eight of the PHAL injection sites (experiments BST10, 25, 29, 26, 41, 46, 64, and 101) are centered in various rostrocaudal regions dorsal to the anterior commissure (Figs. 1, 2A–D, and 3), and the other 10 injection sites (experiments ACB12 and BST13, 86, 97, 102, 103, 112, 114, 134, and 179) are centered in various rostrocaudal regions ventral to the anterior commissure (Figs. 1, 2E–G, and 3). These injection sites overlap to a greater or lesser extent, and together involve most of the BSTam. In all of these experiments, the vast majority of PHAL-labeled neurons are confined to either dorsal or ventral regions of the BSTam, with very few PHAL-labeled neurons in adjacent BST cell groups, including the anterolateral area and oval nucleus (adjacent to the dorsal BSTam), and fusiform, dorsomedial, magnocellular, and ventral nuclei (adjacent to the ventral BSTam) (Figs. 1–3). In several experiments with a PHAL injection centered in the ventral BSTam, a very few PHAL-labeled neurons are also observed in the hypothalamic parastrial nucleus, which lies immediately medial to the ventral BSTam (see Figs. 1–3). Importantly, the overall projection pattern displayed in each of these experiments is virtually identical, although densities of PHAL-labeled axons and terminal boutons vary between experiments, roughly in proportion to the size of the injection sites (Figs. 1–3).

PHAL injections centered in various components of the BST anterolateral group adjacent to the BSTam have been analyzed previously (Dong et al., 2000, 2001b; Dong and Swanson 2003, 2004a), and injections involving the three nuclei (dorsomedial, magnocellular, and ventral) embedded in the BSTam are described in the accompanying two reports (Dong and Swanson, 2005a,b). In addition, the PHAL injection in experiment BST23 is centered in the miniscule dorsal nucleus of the BST—just ventral to the lateral ventricle, between the BST principal nucleus and dorsal BSTam (Fig. 1E). Its projections are described briefly to help clarify its place within the BST.

Overview of BSTam projections

All PHAL injections centered in various regions of the BSTam dorsal and ventral to the anterior commissure label the same basic pattern of axonal projections (Fig. 4). Because of their complexity, it is useful to begin with an overview, followed in the next section with a detailed analysis of pathways and terminal field distribution. Within the BST, each injection centered in a particular region of the BSTam labels abundant axons throughout the rest of the BSTam (Fig. 5A,B), as well as moderate to dense inputs to the fusiform and rhomboid nuclei and caudoventral corner of the anterolateral area; and moderate inputs to the BSTamg dorsomedial, magnocellular, and ventral nuclei. In the BST posterior division they provide moderately dense inputs to the interfascicular nucleus. Other BST components receive light, if any, inputs from the BSTam.

Outside the BST, BSTam projections follow ascending and descending courses to their targets. Major terminal fields of ascending projections include the lateral septal nucleus, nucleus accumbens, and substantia innominata—which are particularly obvious in ventral regions of the lateral septal nucleus (ventral part and the rostral part, ventrolateral zone, ventral region; Fig. 5A,B) and the caudal end of the nucleus accumbens shell region (Fig.

5A′,A″,B′,B″). Via ascending fibers through the stria terminalis and ansa peduncularis, all regions of the BSTam generate abundant terminal boutons in caudal regions of the substantia innominata (Fig. 6A,B) and medial part of the central amygdalar nucleus (Fig. 6A′,B′), and light to moderate inputs to several other amygdalar cell groups, including the anterodorsal part of the medial nucleus, the anterior and posterior basomedial nuclei, and the posterior basolateral nucleus.

Four major pathways descend from BSTam to hypothalamus and lower brainstem (Fig. 4). BSTam axons in the medial forebrain bundle and ventral propriohypothalamic pathway most densely innervate the posterior zone of the lateral hypothalamic area's subfornical region, along with the dorsomedially contiguous dorsomedial hypothalamic nucleus (especially its ventral part) and ventrally contiguous intermediate part of the tuberal nucleus (Fig. 7A′,B′,C,C′,D,D′). For a discussion of the propriohypothalamic pathways see Thompson and Swanson (2003). Farther down the medial forebrain bundle substantial inputs are established in the ventral tegmental area (Fig. 8A,B), retrorubral area, midbrain raphé nuclei, and ventrolateral periaqueductal gray (Fig. 8A′,B′). As described before (Dong et al., 2000,2001b;Dong and Swanson 2003,2004a), all components of the BST anterolateral group contribute heavily to these two pathways, although their inputs to the lower brainstem are considerably denser than those to be described here from the BSTam.

A third group of descending axons courses through the medial propriohypothalamic pathway to innervate densely caudal regions of the medial preoptic nucleus (all parts; Fig. 7A,B), and to innervate moderately the anterior hypothalamic nucleus. Axons from the ventral propriohypothalamic pathway also appear to contribute terminal boutons to the caudal medial preoptic nucleus and adjacent medial preoptic area (Fig. 7A,B). The medial propriohypothalamic pathway also appears to transmit BSTam axons to the periventricular hypothalamic nucleus, subparaventricular zone, and cell-sparse regions surrounding the cellular core of the ventromedial hypothalamic nucleus.

The fourth and largest group of descending BSTam axons courses through the periventricular propriohypothalamic pathway to regions adjacent to the third ventricle. As described in the next section, BSTam neurons closest to the anterior commissure appear to innervate most densely the hypothalamic periventricular region.

Ipsilateral BSTam projection pathways

The axonal projections and terminal fields displayed in experiment BST10 are analyzed in detail because the injection site has the least contamination outside the limits of the BSTam, and because the results are representative of the overall projection pattern observed from all regions of the BSTam. Minor differences between experiments are dealt with afterward. The vast majority of PHAL-labeled neurons in experiment BST10 lie rostrally and in the central core of the dorsal BSTam, with a very few PHAL-labeled neurons extending laterally into the adjacent BST anterolateral area (Figs. 1, 2A, and 3).

Local projections—Within the BST, abundant PHAL-labeled axons from the injection site generate many terminal boutons throughout most of the dorsal BSTam (Fig. 9E–H). Only scattered axons from the dorsal BSTam extend into the adjacent anterolateral area and oval nucleus (Fig. 9E–H), although these two cell groups are surrounded by abundant labeling from the injection site. Instead, many PHAL-labeled axons arch medially (Fig. 9E–G) or laterally (Fig. 9H,I) around the medial or lateral edges, respectively, of the anterior commissure to enter the ventral BSTam, where they generate branches and terminal boutons everywhere (Fig. 9E–I). A dense terminal plexus is also labeled in the nearby fusiform nucleus (Fig. 9G,H) and caudal end of the anterolateral area (Fig. 9I,J). Moderately dense

inputs are observed in the rhomboid, dorsomedial, magnocellular, and ventral nuclei (Fig. 9I,J).

In the BST posterior division (Fig. 9K,L) many labeled fibers extend through the transverse and interfascicular nuclei, where they branch frequently and generate many boutons. The principal nucleus contains only scattered fibers and boutons from the BSTam (Fig. 9J,K).

Rostral ascending pathway—Many axons leave the rostral end of the dorsal BSTam to enter directly the nucleus accumbens, where a dense terminal field is established in the adjacent caudal ("septal") pole (Figs. 5A′,B′ and 9D). Just rostral to this, PHAL-labeled axons also generate a clear terminal field in dorsal and ventral regions of the accumbens "shell" (Fig. 9C), although many fewer axons extend into the more rostral shell region (Fig. 9A,B). However, many labeled axons turn ventrally and generate substantial terminal boutons in the medial olfactory tubercle (Fig. 9B,C) and rostral substantia innominata (Fig. 9C,D). In addition, many PHAL-labeled axons extend directly into the substantia innominata from the region of the ventral BSTam and nearby fusiform nucleus (Fig. 9E–J). Dense terminal fields are observed in a region of the substantia innominata immediately adjacent to the BST, and in an isolated pathway extending through roughly the middle of the substantia innominata (Fig. 9E–J).

Another group of BSTam axons extends dorsally into the adjacent lateral septal complex (Fig. 9D–I), where moderate to dense inputs are observed in the ventral part (LSv), and ventral regions of the rostral part (LSr.m.v.r, LSr.m.v.c, and LSr.vl.v) (Figs. 5A,B and 9D–H). The rest of the lateral septal complex contains at most scattered fibers (Fig. 9B–J). A few labeled axons course through the rostral end of the lateral septal nucleus to end in deep layers of the infralimbic and prelimbic areas of the medial prefrontal cortex (Fig. 9A).

Stria terminalis and ansa peduncularis—PHAL-labeled axons extend dorsally from the caudal end of the dorsal BSTam to enter the stria terminalis (Fig. 9H–J), and then course caudally through intermediate regions of the stria to enter the amygdalar region (Fig. 9J–S), where they merge imperceptibly with the vast majority of BSTam axons to the amygdalar region, which arrive via the ansa peduncularis (Fig. 4). Initially, the vast majority of the latter display abundant branching and terminal boutons in caudal regions of the substantia innominata (Figs. 6A,B and 9I–K). This uninterrupted terminal field extends caudally through the substantia innominata before entering the central amygdalar nucleus (Fig. 9L–P). The medial part of the central nucleus is most densely innervated, whereas the capsular and lateral parts are only lightly innervated (Figs. 6A′,B′ and 9M–R). Scattered fibers and terminal boutons are also observed in several other amygdalar cell groups, including the anterodorsal part of the medial nucleus, anterior and posterior parts of the basomedial nucleus, posterior basolateral nucleus, and posterior nucleus (Fig. 9M–X). A few axons and terminal boutons are found in the ventral subiculum and entorhinal area (Fig. 9U–X), components of the hippocampal formation.

Descending projections to hypothalamus—As outlined in the preceding section, PHAL-labeled BSTam axons reach the hypothalamus through four relatively distinct pathways (Fig. 4).

Periventricular propriohypothalamic pathway: The vast majority of BSTam axons enter the hypothalamic periventricular region ventral to the crossing of the anterior commissure by coursing initially through the BST dorsomedial nucleus (Fig. 9I,J). Then they travel ventrally and caudally near the third ventricle to innervate the periventricular, paraventricular, and arcuate nuclei (Fig. 9I–W). Abundant terminal boutons are generated in the preoptic, anterior, and intermediate parts of the periventricular nucleus (Figs. 7A,A′,B,B

′,C,D and 9I–T). In the paraventricular hypothalamic nucleus, PHAL-labeled axons provide moderate to dense inputs to the periventricular and anterior parvicellular parts (Figs. 9K–M and 10A,B). In the dorsal medial parvicellular part a moderately dense terminal field is restricted to the rostral end (at the level of Fig. 9N; also see Fig. 10C,D), with very sparse axons more caudally (Figs. 9O,P and 10E,F). At this level, a dense cluster of PHAL-labeled terminal boutons is found medially in the juxtaparaventricular region of the lateral hypothalamic area (Figs. 9N and 10C,D). The latter does not appear to arise from the periventricular pathway. Instead, incoming fibers course through the BST posterior division to enter the lateral hypothalamic area directly.

In the paraventricular nucleus magnocellular division, the anterior part and the rostral end of the medial zone of the posterior part receive light to moderate BSTam inputs (Figs. 9K,N and 10A,C) whereas the lateral zone of the posterior part contains only scattered fibers (Figs. 9O and 10E). PHAL-labeled axons with prominent boutons are also present in the rostral end of the dorsal and ventral medial parvicellular parts of the paraventricular nucleus (Figs. 9N and 10C–E). In contrast, the caudal end of the dorsal parvicellular part, the lateral parvicellular part, and the forniceal part contain only scattered fibers (Figs. 9P and 10E,F).

Many BSTam axons also extend ventrally and caudally to provide dense inputs to the arcuate nucleus (Figs. 9O–S and 10G,H), and the region in and around the posterior part of the periventricular nucleus (Figs. 9T–V and 10I). In the former, a very dense terminal plexus is concentrated dorsomedially, with only scattered fibers extending ventrolaterally (Figs. 9O–S and 10G,H).

Medial propriohypothalamic pathway: Overall, this pathway extends through the medial hypothalamic nuclei. Axons from the BSTam only extend a short distance though the rostral end of the pathway, most notably to a distinct terminal field in caudal regions of the medial preoptic nucleus (Fig. 4). Actually, labeled axons reach the medial preoptic nucleus by at least two distinct routes. One group arches medially and ventrally from the injection site, through rostral regions of the lateral preoptic area to enter dorsal regions of the medial preoptic area dorsal to the medial preoptic nucleus (Fig. 9E–J). Before entering dorsal regions of the medial preoptic nucleus they branch frequently in rostral regions of the lateral preoptic area (Fig. 9D–H), anterodorsal preoptic nucleus (Fig. 9G,H), and parastrial nucleus (Fig. 9F–H).

The other group of PHAL-labeled axons courses through the BST magnocellular and ventral nuclei initially to enter the medial preoptic area (Fig. 9I,J), where they present a dense terminal plexus, especially ventrally (Fig. 9H–K), along with a more moderate terminal field in the nearby anteroventral preoptic nucleus (Fig. 9H,I). Then this fiber group divides into a caudally directed component that joins the ventral propriohypothalamic pathway (see next section) and a medially directed component that enters and contributes to a distinct terminal field in caudoventral regions of the medial preoptic nucleus (Fig. 9J).

Thus, BSTam axons take both dorsal and ventral routes to converge on a terminal field in the caudal end of the medial preoptic nucleus (Fig. 9K,L). At these levels, abundant axonal branches and terminal boutons are distributed throughout the medial and lateral parts of the nucleus, although the terminal field in the medial part tends to be denser (see Fig. 7A,B). This curious terminal field begins at the level of the rostral tip of the suprachiasmatic nucleus, in ventral regions of the medial and lateral parts of the medial preoptic nucleus (Fig. 9J).

It is likely that the medial propriohypothalamic pathway also contributes to BSTam terminal fields in the subparaventricular zone and more caudal levels of the periventricular nucleus

(Fig. 9L–O). Remaining axons in the medial propriohypothalamic pathway extend caudally and ventrally through the anterior hypothalamic nucleus (Fig. 9M,N), ending finally in the cell sparse internuclear area between the dorsomedial and ventromedial hypothalamic nuclei (Fig. 9O–R). The central part of the anterior hypothalamic nucleus receives a moderate input from the BSTam (Fig. 9M), and a few BSTam axons are observed within the nucleus circularis (Fig. 9M), a distinct cluster of oxytocinergic magnocellular neurosecretory neurons within the anterior hypothalamic nucleus.

Ventral propriohypothalamic pathway: As just mentioned, a group of BSTam axons traveling through the medial preoptic area joins this pathway (Fig. 4), which extends along the base of the hypothalamus. At anterior hypothalamic levels most axons in this pathway resemble fibers of passage (Figs. 7A,B and 9L–O), but then a number of them turn medially to branch and generate terminal boutons in the retrochiasmatic area (Fig. 9M,N), whereas a few others turn laterally to form sparse terminal boutons just dorsal to the supraoptic nucleus, in the ventral zone of the lateral hypothalamic area, anterior region (Fig. 9K–N). The supraoptic nucleus itself receives only a very sparse input (Fig. 9K–N).

Most PHAL-labeled axons in this pathway begin to ramify at tuberal levels. They generate moderate to dense terminal fields in the tuberal nucleus itself, before arching dorsally to generate a dense terminal plexus (branches and boutons) centered in the posterior zone of the lateral hypothalamic area, subfornical region (Fig. 9P–T). This dense terminal field extends dorsomedially to merge with terminals immediately surrounding the column of the fornix, arising in part from the medial forebrain bundle (see next section), and with terminals in the dorsomedial nucleus, especially its ventral part (Fig. 9S,T). These dorsomedially directed fibers contribute to very rich branching and boutons in the caudal end of the dorsomedial nucleus and in the immediately adjacent ventral zone of the lateral hypothalamic area, juxtaventromedial region (Fig. 9S,T). Caudal to the dorsomedial nucleus, this terminal field lies in the intranuclear area of the hypothalamic periventricular region adjacent to the posterior periventricular nucleus (Fig. 9U).

Another distinct terminal field arising from this ventral pathway lies in the terete subnucleus of the tuberal nucleus (Fig. 9S–U). Remaining fibers generate a few terminal boutons in the ventral tuberomammillary nucleus (Fig. 9V,W) before traveling through the mammillary body capsule, arching medially through the posterior hypothalamic nucleus, and entering the periaqueductal gray (Fig. 9X).

Medial forebrain bundle: Many axons from the BSTam enter the lateral hypothalamic area from caudodorsal regions of the substantia innominata and lateral preoptic area (Fig. 9I–K). In transverse histological sections they are cut in cross-section and display few boutons in the lateral preoptic area and anterior region of the lateral hypothalamic area (Fig. 9I–L). This descending fascicle lies in a restricted intermediate region of the lateral hypothalamic area (Fig. 9M–V).

Whereas medial forebrain bundle axons from the BST anterolateral group densely innervate the forniceal part of the paraventricular nucleus (Dong et al., 2001b; Dong and Swanson 2003, 2004a), those from the BSTam terminate only lightly there (Fig. 9O). However, the BST anterolateral group and BSTam both innervate periforniceal regions of the lateral hypothalamic area at tuberal levels. Just caudal to the paraventricular nucleus many BSTam axons start to ramify and generate a dense terminal plexus in the suprafornical region and adjacent territories of the juxtadorsomedial region of the lateral hypothalamic area, essentially between the column of the fornix and zona incerta (Figs. 7A″,B′ and 9Q–S). Some of these fibers appear to extend ventral to the fornix to merge with the terminal field, described above, centered in the posterior zone of the lateral hypothalamic area's subfornical

region and also formed by the ventral pathway (Fig. 9Q–S). Many of these axons extend medially to generate boutons in the anterior and ventral parts of the dorsomedial nucleus (Figs. 7A′,B′ and 9R,S), which also receive contributions from the ventral pathway. In addition, some fibers in the suprafornical terminal field continue dorsally through the zona incerta and posterior hypothalamic nucleus to enter the dorsal thalamus (Fig. 9N–T). Very few terminal boutons are observed in the posterior hypothalamic nucleus (Fig. 9S–U).

Remaining PHAL-labeled axons in the medial forebrain bundle maintain an intermediate position in the lateral hypothalamic area (Fig. 9Q–W) and generate many branches and terminal boutons in the caudal end of the hypothalamus (Fig. 9V,W). Specifically, before entering the midbrain, moderate numbers of fibers turn medially to generate a distinct terminal field in the lateral part of the supramammillary nucleus (Fig. 9W).

Thalamic input—BSTam axons enter the rostral thalamus directly and generate a few terminal boutons in rostral levels of the paraventricular nucleus and nucleus reuniens, and in the paratenial nucleus (Fig. 9K–M). Throughout the length of the hypothalamus axons in both the periventricular pathway and medial forebrain bundle leave and extend dorsally into the thalamus (Fig. 9L–U). The densest terminal fields are observed in caudal regions of the paraventricular nucleus and the adjacent medial part of the mediodorsal nucleus (Fig. 9T,U). Light to moderate inputs are also observed in the intermediodorsal and central medial nuclei, nucleus reuniens, and medial regions of the lateral habenula (Fig. 9O–V).

Projections to lower brainstem—BSTam axons follow three pathways through the midbrain and hindbrain. A small number course through the posterior hypothalamic nucleus to enter and continue through the periaqueductal gray (Fig. 9W,X) before ending in the pontine central gray (Figs. 4 and 9X–AA). Along this pathway only a few terminal boutons are observed in the medial division of the periaqueductal gray (Fig. 9AA).

The vast majority of descending axons follow the medial forebrain bundle into the ventral tegmental area (Fig. 9X,Y), where substantial terminal boutons are observed (see Fig. 8A,B). Axons emerging from the ventral tegmental area then take either a median or a lateral branch (Fig. 9X–AA). The former displays a few terminal boutons in the interfascicular, central linear, and dorsal nuclei of the raphé (Fig. 9Y–AA), and in the interpeduncular nucleus (Fig. 9Z). The lateral branch courses through the midbrain reticular nucleus and its retrorubral area and then arches dorsomedially to enter the ventrolateral division of the periaqueductal gray (Fig. 9Y–AA). There are a substantial number of terminal boutons in the retrorubral area (Fig. 9Z).

PHAL-labeled axons from the three routes just described converge in the ventrolateral division of the periaqueductal gray (Fig. 9AA), where there is a moderately dense terminal field (also see Fig. 8A′,B′). The remaining axons extend caudally into the pontine central gray and generate scattered terminal boutons in the lateral tegmental nucleus, Barrington's nucleus, and rostral end of the locus ceruleus (Fig. 9BB). A few BSTam axons also course laterally to generate scattered terminals in the parabrachial nucleus (Fig. 9BB). Finally, a very few axons turn ventrally to enter the pontine reticular nucleus and then extend caudally to end in the medial part of the nucleus of the solitary tract and parvicellular reticular nucleus (Fig. 9CC,DD).

Contralateral projections

The BSTam generates only light contralateral projections, most of which emerge from the medial forebrain bundle and mirror the ipsilateral pattern. A few axons cross the midline in regions immediately surrounding the anterior commissure, and they generate a few terminal boutons in the contralateral BST, nucleus accumbens, and lateral septal nucleus (Fig. 9C–J).

Some of these axons continue through the contralateral ansa peduncularis (in the substantia innominata) to end in the medial part of the central amygdalar nucleus (Fig. 9K–P). Along the entire length of the hypothalamus scattered axons cross the midline dorsal and ventral to the third ventricle and they give rise to scattered terminal boutons in hypothalamic regions densely innervated on the ipsilateral side, including the medial preoptic and lateral hypothalamic areas, and the periventricular, paraventricular, arcuate, and dorsomedial nuclei (Fig. 9I–W). In the thalamus the only obvious contralateral projection consists of a few labeled axons in the paraventricular nucleus (Fig. 9L–U), and in the lower brainstem there are sparse contralateral inputs to the ventral tegmental area, retrorubral area, ventrolateral division of the periaqueductal gray, and lateral tegmental nucleus (Fig. 9W–BB).

Other BSTam regions

By and large the overall projection pattern labeled in each BSTam injection site illustrated in Figures 1–3 is the same. Variations in the absolute staining intensity for a particular experiment are consistent with differences in the size of the PHAL injection site, the extent to which the injection site spread in a very limited way to adjacent cell groups, or gradients of projection strength within the BSTam itself (for example, there is a cell condensation in intermediate regions of the dorsal BSTam; see *Nomenclature* section above). Nevertheless, it may be worth noting that denser projections to the hypothalamic periventricular region are observed consistently with injection sites centered rostroventrally in the dorsal BSTam (e.g., experiments BST10, 25, and 46) and rostrodorsally in the ventral BSTam (e.g., experiments ACB12, BST114, and BST134)—that is, in BSTam regions immediately adjacent to the anterior commissure.

The only exception involved experiment ACB12, which labeled the most extensive expanse of the ventral BSTam, and was the only experiment that labeled neurons in the rostral tip of the ventral BSTam (Figs. 1, 2G, and 3). The overall projection pattern (see Figs. 4–8), including inputs to the hypothalamic periventricular region, are similar to those labeled in other BSTam experiments, except for several distinct terminal fields associated with the neuroendocrine system that are different from, or not observed in, the other experiments (Fig. 11). First, as in the other experiments, dense PHAL labeling is observed in the periventricular part, anterior parvicellular and magnocellular parts, and rostral regions of the dorsal zone of the medial parvicellular part (compare Figs. 11A,A′ and11B,B′). Second, in experiment ACB12 much denser inputs are labeled to both the medial and lateral zones of the posterior magnocellular part of the paraventricular nucleus (compare Figs. 11B,C and 11B′,C′), and to the supraoptic nucleus. In the lateral zone of the posterior magnocellular part of the paraventricular nucleus, PHAL labeling is concentrated medially (Fig. 11C′). Third, in experiment ACB12 the input to caudal regions of the dorsal zone of the medial parvicellular part of the paraventricular nucleus is more densely labeled than in the other experiments (compare Fig. 11Cand C′). And fourth, a distinct terminal field in the nucleus circularis is labeled in experiment ACB12 (Fig. 12A, A′).

There are two obvious explanations for these observations, which require further analysis with retrograde tracing methods to clarify. First, a unique cell type in the rostroventral BSTam may generate these projections to the region of neuroendocrine motoneuron pools, and second the projections may arise from labeled neurons in the adjacent parastrial nucleus. The latter reportedly projects to the medial zone of the posterior magnocellular part of the paraventricular nucleus and the dorsal zone of the medial parvicellular part of the paraventricular nucleus, and to the supraoptic nucleus, but possibly not to the nucleus circularis (Thompson and Swanson, 2003).

BST dorsal nucleus projections

This tiny yet distinct group of tightly packed neurons is embedded in the caudal tip of the dorsal BSTam, adjacent to the rostral tip of the BST posterior division's principal nucleus, just ventral to the lateral ventricle (Fig. 1). Based on rather inconclusive cyto- and chemoarchitectonic criteria the BST dorsal nucleus (BSTd) was provisionally assigned to the BST posterior division (Ju and Swanson, 1989;Ju et al., 1989). Fortunately, one of the over 200 PHAL injection sites involving the BST is centered in the BSTd, with only a few labeled neurons spreading into adjacent regions of the dorsal BSTam (experiment BST23; Figs. 1C–E and 13). It seems worth describing the results in enough detail to establish whether its projection pattern is unique, similar to the BSTam, or similar to the BST principal nucleus.

Within the BST anterior division, the BSTd provides dense inputs to the entire BSTam, anterolateral area, and fusiform nucleus; moderate inputs to the magnocellular, dorsomedial, and ventral nuclei, and light inputs to the oval, juxtacapsular, and rhomboid nuclei. In the BST posterior division, the BSTd projects massively to the interfascicular and transverse nuclei, but only lightly to the principal nucleus. Interestingly, BST23 is the only experiment in our extensive PHAL library that labels a dense input to the strial extension of the BST posterior division.

A rostral projection from the BSTd innervates densely ventral regions of the lateral septal nucleus (the LSv and LSr.vl.v) and the caudal pole and shell of the nucleus accumbens; and innervates moderately the olfactory tubercle and rostral regions of the substantia innominata.

PHAL-labeled axons from the BSTd also course through the stria terminalis and ansa peduncularis to the amygdalar region. Associated with this, a massive terminal plexus is observed in caudodorsal regions of the substantia innominata and in the central and medial amygdalar nuclei (the BSTam projects only to the central nucleus). In the medial amygdalar nucleus dense inputs are observed in the anterodorsal part and layers b and c of the posterodorsal part, and there is a light input to the posteroventral part. The BSTd also provides light to moderate inputs to the anterior and posterior basomedial nuclei, posterior nucleus, and cortical nucleus of the amygdala, as well as to ventral regions of the subiculum and field CA1, and the entorhinal area, of the hippocampal formation.

BSTd axons descend through the medial and ventral propriohypothalamic pathways and the medial forebrain bundle. Unlike the BSTam, the only significant BSTd input to the hypothalamic periventricular region is to the anterior parvicellular part of the paraventricular nucleus. At preoptic levels, the BSTd generates dense terminal fields in the rostral lateral preoptic area and in the medial preoptic area.

Like the BST principal nucleus (Gu et al., 2003; Dong and Swanson, 2004b), BSTd axons in the medial propriohypothalamic pathway innervate densely the anteroventral periventricular nucleus, medial preoptic nucleus (all three parts, with the strongest input to the lateral), tuberal nucleus, and ventral premammillary nucleus—although its inputs to the ventrolateral part of the ventromedial nucleus are very sparse. And like the BST interfascicular nucleus (Dong and Swanson, 2004b), the BSTd projects densely to the anterior hypothalamic nucleus but not the dorsomedial part of the ventromedial nucleus—or to the dorsal premammillary nucleus, where only a light input is observed.

Like the BST interfascicular and principal nuclei (Dong and Swanson, 2004b), BSTd axons in the ventral propriohypothalamic pathway establish a moderate input to the retrochiasmatic area, a dense input to the subparaventricular zone, and very dense inputs to the juxtaventromedial region of the lateral hypothalamic area and ventrally adjacent

intermediate part of the tuberal nucleus. Axons from this pathway also contribute inputs to the dorsomedial and posterior hypothalamic nuclei.

BSTd axons in the medial forebrain bundle generate terminal boutons in the anterior region of the lateral hypothalamic area but very few elsewhere in this area. The vast majority of axons in this pathway enter the midbrain.

Within the thalamus, the BSTd provides clear inputs to the paraventricular nucleus, nucleus reuniens, and lateral habenula. Caudal to the interbrain, axons remaining in the medial forebrain bundle innervate the midbrain reticular nucleus and its retrorubral area, and the ventrolateral division of the periaqueductal gray.

Overall, the projection pattern for the BSTd revealed in experiment BST23 is quite distinct from that labeled by PHAL injections centered in the BSTam, resembling more the projection pattern established by BST posterior division nuclei (Dong and Swanson, 2004b).

DISCUSSION

This is the first systematic examination of axonal projections from the BSTam and the results suggest that all regions of this relatively undifferentiated component of the BST anterior division generate virtually the same overall pattern of outputs—most prominently to the lateral septal nucleus, ventral striatopallidal system, central amygdalar nucleus, and various components of the hypothalamus. The BSTam, along with the adjacent dorsomedial nucleus of the BSTamg (Dong and Swanson 2005a), appear to generate the most prominent BST inputs directly to the region of hypothalamic neuroendocrine secretomotoneuron pools, with the former being the only anterior division generating obvious projections to the arcuate nucleus.

Earlier literature

The first anterograde tracing study involving the BSTam was based on a large ^{3}H-amino acid injection labeling neurons in both the BSTam and BST anterolateral area (Swanson and Cowan, 1979). Many BSTam terminal fields described here with PHAL were mentioned in the earlier report, including those in the nucleus accumbens shell, substantia innominata, and central amygdalar nucleus; the paraventricular, arcuate, dorsomedial, and posterior periventricular hypothalamic nuclei; the medial preoptic, anterior hypothalamic, and lateral supramammillary nuclei; the lateral hypothalamic area; the paraventricular and paratenial thalamic nuclei and lateral habenula; and the ventral tegmental area, midbrain reticular nucleus and its retrorubral area, periaqueductal gray, and parabrachial nucleus.

Many retrograde tracer studies also confirm BSTam projections described here, although their interpretation is confounded by the possibility of tracer uptake by fibers of passage. (1) Labeled neurons were found in the BSTam after tracer injection in the lateral septal nucleus (Risold and Swanson, 1997), nucleus accumbens (Brog et al., 1993), substantia innominata (Grove, 1988), and central amygdalar nucleus (Cassell et al., 1999). (2) Evidence for a projection from the BSTam to the paraventricular hypothalamic nucleus has been adduced with retrograde tracers by Sawchenko and Swanson (1983), Cullinan et al. (1993), Moga and Saper (1994), Prewitt and Herman (1998), and Spencer et al. (2005); and with anterograde tracing by Risold et al. (1997). A projection to the arcuate nucleus was reported by Zaborsky (1982). (3) We confirmed previous retrograde tracer reports of BSTam projections to the medial preoptic nucleus (Simerly and Swanson, 1986), dorsomedial hypothalamic nucleus (Thompson and Swanson, 1998), "perifornical region" of the lateral hypothalamic area at tuberal levels (Allen and Cechetto, 1993), and lateral supramammillary nucleus (Gonzalo-Ruiz et al., 1992). (4) Retrograde labeling in the BSTam region has been

reported after thalamic injections involving the paraventricular nucleus and the adjacent medial part of the mediodorsal nucleus (Groenewegen and Russchen, 1984; Groenewegen, 1988; Chen and Su, 1990) and lateral habenula (Li et al., 1993). (5) Previous retrograde tracer studies also suggested the existence of BSTam projections to the ventral tegmental area (Phillipson, 1979), retrorubral area (Berendse et al., 1992), and laterodorsal tegmental nucleus (Satoh and Fibiger, 1986). After tracer injections in the periaqueductal gray (Gray and Magnuson, 1992), many fewer retrogradely labeled neurons were observed in the BSTam than in the "ventral and posterior lateral" region of the BST, in agreement with our PHAL results.

Functional implications: projection targets

Projections to neuroendocrine system—Overall projection patterns to the hypothalamic periventricular region from throughout the BSTam (with the possible exception of the rostroventral tip) are indistinguishable, although they do appear to be somewhat denser from regions adjacent to the anterior commissure. Dense projections to the arcuate and posterior periventricular nuclei are the most distinguishing features of BSTam projections to the periventricular region (Fig. 14). In the former a very dense terminal plexus is centered dorsomedially, where most dopamine neuroendocrine motoneurons, which inhibit prolactin release, are concentrated (see Markakis and Swanson, 1997), with a much lighter input to ventrolateral regions, where neurons synthesizing growth hormone-releasing hormone are concentrated (Sawchenko et al., 1985).

The BSTam also innervates moderately densely the hypothalamic region (anterior periventricular nucleus and periventricular part of the paraventricular nucleus; see Markakis and Swanson, 1997) where parvicellular neuroendocrine somatostatin neurons are concentrated. Most parvicellular neurosecretory neurons synthesizing corticotropin-releasing hormone and thyrotropin-releasing hormone are found in the dorsal medial parvicellular part of the paraventricular nucleus (see Markakis and Swanson, 1997), and curiously, BSTam inputs are concentrated only in the rostral end of this cell group.

The BSTam also innervates lightly to moderately regions of the magnocellular neuroendocrine system where oxytocinergic neurons predominate, most obviously in the medial zone of the posterior magnocellular part of the paraventricular nucleus (see Swanson, 1986). It remains to be demonstrated ultrastructurally whether BSTam axons synapse on neuroendocrine oxytocinergic neurons there, and it should be noted that most of the BSTam clearly provides very little input to the supraoptic nucleus, which contains a major population of neuroendocrine oxytocinergic neurons.

BSTam projections are also positioned to influence neuroendocrine system output via several indirect routes. First, a BSTam input to the lateral hypothalamic area's juxtaparaventricular region could innervate GABAergic neurons with short projections to the paraventricular nucleus (Roland and Sawchenko, 1993; Herman et al., 2002). Second, most components (dorsomedial, parastrial, anterodorsal preoptic, and anteroventral preoptic nuclei) of the recently defined hypothalamic visceromotor pattern generator network (Thompson and Swanson, 2003) receive moderate to dense inputs from the BSTam. Third, the BSTam innervates the medial part of the medial preoptic nucleus, which projects extensively to the periventricular region (Simerly and Swanson, 1988). And fourth, the BSTam innervates substantially a number of cerebral nuclei (components of the "basal ganglia")—including the fusiform, dorsomedial, and magnocellular BST nuclei and the ventral part of the lateral septal nucleus—that send topographically organized projections to the neuroendocrine system (Risold and Swanson, 1997; Dong et al., 2001b, Dong and Swanson, 2005a,b).

Projections to preautonomic cell groups—Compared to the BST anterolateral group, the BSTam provides only very light inputs to the hindbrain nucleus of the solitary tract and parabrachial nucleus. The BSTam does provide relatively light to moderate inputs to the dorsal (rostrally) and ventral medial parvicellular parts of the paraventricular hypothalamic nucleus. The former projects to the entire preganglionic autonomic neuron system of the spinal cord (sympathetic and parasympathetic), whereas the latter does the same, and also innervates heavily the dorsal vagal complex (Swanson and McKellar, 1979; Swanson and Kuypers, 1980). The BSTam also projects to two regions of the lateral hypothalamic area with neurons that project to the dorsal vagal complex and spinal preautonomic regions: the dorsal region (Saper et al., 1976; Swanson and Kuypers, 1980) and retrochiasmatic area (Saper et al., 1976; Ribeiro-Barbosa et al., 1999). However, these two regions are quite heterogeneous, and the exact cell type(s) innervated by the BSTam remains to be established.

BSTam projections are also in a position to influence autonomic responses in several indirect ways. First, the components of the hypothalamic visceromotor pattern generator network that are innervated by the BSTam (the dorsomedial, parastrial, anterodorsal preoptic, and anteroventral preoptic nuclei; see above) in turn send dense projections to the preautonomic parts of the paraventricular hypothalamic nucleus, in addition to specific neuroendocrine secretomotoneuron pools (Thompson and Swanson, 2003). Second, as reviewed recently, the central amygdalar nucleus and BST anterolateral group, which receive major inputs from the BSTam, may be regarded as a component of the striatopallidal system specialized for the cerebral modulation of autonomic responses (Swanson, 2000, 2003; Dong and Swanson 2003, 2004a). And third, the BST am projects to the BST dorsomedial, magnocellular, and ventral nuclei, which in turn also send dense projections to the paraventricular autonomic parts, and to Barrington's nucleus, which sends descending projections to sacral parasympathetic regions (see Dong and Swanson, 2005a,b).

Projections to behavior control column—Several components of the behavior control column in medial regions of the upper brainstem (Swanson, 2000; Thompson and Swanson, 2003) receive inputs from the BSTam. First, the lateral part of the medial preoptic nucleus, which is thought to play a role in the expression of masculine sexual behavior, receives a selective input to its caudal tip from the BSTam. Whether the caudal end of the lateral part of the medial preoptic nucleus actually participates in controlling masculine sexual behavior remains to be determined experimentally. Second, the anterior hypothalamic nucleus, which modulates defensive behavioral responses, receives a light projection from the BSTam. Third, the descending division of the paraventricular hypothalamic nucleus is a key part of the ingestive behavior controller (as well as projecting to brainstem and spinal preautonomic cell groups, as discussed above), and it receives a substantial input from the BSTam. In this regard, it should be noted that the BSTam also innervates heavily the arcuate nucleus, which in addition to classical neuroendocrine functions (see above) has been implicated clearly in the regulation of ingestive behavior, probably via projections to the paraventricular nucleus and adjacent regions of the lateral hypothalamic area (see Sawchenko, 1998; Elmquist et al., 1999; Schwartz et al., 2000; Swanson, 2000; Watts, 2001), which may also receive inputs from the BSTam. There is experimental evidence to suggest that the BSTam itself plays a role in mechanisms underlying anorexia (Ciccocioppo et al., 2003). And fourth, the ventral tegmental area participates in the control of locomotor behavior (among other functions), and it is innervated relatively lightly by the BSTam, which, however, also projects substantially to the nucleus accumbens and substantia innominata—two parts of the ventral striatopallidal system that project to the ventral tegmental area as part of the system that controls locomotor behavior expression (for review see Swanson, 2000). In addition, medial (shell) regions of the nucleus accumbens have been implicated in the control of feeding behavior (see Stratford and Kelley, 1997, 1999). The exact functional role of BSTam

projections to the nucleus accumbens, substantia innominata, and ventral tegmental area remain to be clarified.

Projections to the behavioral state control system—The supramammillary nucleus is innervated by the BSTam, and its projections to the medial septal complex and hippocampal formation are involved in modulating hippocampal theta rhythm, which is correlated with behavioral state (exploratory or locomotor behavior; see Vertes, 1992; Vertes and Kocsis, 1997). In addition, the tuberomammillary nucleus, which is the only neuronal source of histamine in the central nervous system (see Köhler et al., 1985), receives an input from the BSTam. The functional significance of BSTam projections to the lateral hypothalamic area is obscure and requires experimental analysis.

Projections to thalamocortical feedback loops—Like the BST anterolateral group, the BSTam projects to several components of the midline, medial, and intralaminar groups of the thalamus (including the paraventricular nucleus, intermediodorsal nucleus, and nucleus reuniens; medial part of the mediodorsal nucleus, and central medial nucleus). As reviewed elsewhere (Risold et al., 1997; Dong and Swanson, 2003), these thalamic cell groups establish widespread, topographically organized projections to a continuous expanse of cerebral cortex that includes the anterior cingulate area, prelimbic and infralimbic areas of the prefrontal region, agranular insular area, perirhinal area of the ventral temporal region, and entorhinal area and ventral subiculum of the hippocampal formation.

Functional implications: neural inputs

To clarify further the functional significance of the present results it is important briefly to consider reported sources of major neural inputs to the BSTam. Overall, it appears that of all BST cell groups, the BSTam receives the most diverse set of inputs. Thus, it is in a strategic position to integrate neural inputs from the cerebral hemisphere, thalamus, hypothalamus, and lower brainstem.

Cortico-striatopallidal inputs—The BSTam (especially pronounced dorsally) receives massive direct inputs from both the central and the medial amygdalar nuclei (Sun et al., 1991; Dong et al., 2001a), and they are presumably modified by direct inputs from the BST anterolateral group (Dong et al., 2000, 2001b; Dong and Swanson, 2003, 2004a) and BST posterior division (Dong and Swanson, 2004b), which in turn receive massive inputs from the central and medial amygdalar nuclei, respectively (and brainstem viscerosensory nuclei; see references just cited). As reviewed elsewhere (Dong and Swanson, 2003, 2004a), the central amygdalar nucleus and BST anterolateral group together receive their most dense cortical inputs from the primary gustatory and visceral sensory areas, from visceral association areas (in the agranular insular region), from secondary main olfactory sensory areas (mainly in the amygdalar region), from the prefrontal region, and from the ventral subiculum of the hippocampal formation (also see McDonald, 1998). In turn, the central amygdalar nucleus and BST anterolateral group send their most dense projections to brainstem regions modulating autonomic and somatomotor responses. Thus, the central amygdalar nucleus and BST anterolateral group may be viewed as forming part of a cortico-striatopallidal system specialized for coordinating autonomic and somatomotor responses associated especially with ingestive behaviors (also see Swanson, 2003). In contrast, the medial amygdalar nucleus and BST posterior division receive major inputs from the accessory olfactory system, and may be viewed as forming part of a cortico-striatopallidal system specialized for controlling reproductive and defensive behaviors, the two major classes of social behaviors. The BSTam receives inputs from the central and medial amygdalar nuclei and may be viewed as forming part of a cortico-striatopallidal system specialized for coordinating neuroendocrine responses with autonomic and somatomotor

responses associated with ingestive behaviors, especially those associated with energy balance (Fig. 14).

The BSTam (again most prominent dorsally) receives substantial direct inputs from the ventral subiculum (Canteras and Swanson, 1992; Dong et al., 2001a) and ventral field CA1 (Lee Cenquizca and Larry W. Swanson, personal communication) of the hippocampal formation, as well as light inputs from ventral regions of the lateral septal nucleus (Risold and Swanson, 1997), which in turn receive dense inputs from Ammon's horn (including field CA1) and the subiculum (see Swanson and Cowan, 1977). Thus, information processed in ventral components of the intrahippocampal (trisynaptic) circuit may reach directly and indirectly the BSTam. The BSTam has been shown to relay information from the region of the ventral subiculum to the paraventricular hypothalamic nucleus (Cullinan et al., 1993; Herman and Cullinan, 1997).

Finally, it is clear that the infralimbic area of the ventromedial prefrontal region projects directly to the BSTam (Hurley et al., 1991; Dong and Swanson, 2001a).

Brainstem viscerosensory inputs—The BSTam appears to receive direct inputs from caudal regions of the nucleus of the solitary tract (Ricardo and Koh, 1978) and lateral division of the parabrachial nucleus (Alden et al., 1994), suggesting that information related to viscerosensation and/or nociception reaches the BSTam. The medial division of the parabrachial nucleus also sends projections to the region of the BSTam (Alden et al., 1994), suggesting that it may receive gustatory information directly from the brainstem (see Herbert et al., 1990). In addition, neurons immunoreactive for galanin-like peptide—which are restricted to the arcuate nucleus, and most of which express leptin receptors—project to the region of the BSTam (Takatsu et al., 2001).

Viscerosensory information potentially can reach the BSTam via many indirect routes. One of the more obvious is the hypothalamic visceromotor pattern generator network (Thompson and Swanson, 2003), each of whose major nodes projects to the BSTam. Another possibility includes the paraventricular and paratenial thalamic nuclei (Weller and Smith, 1982; Berendse and Groenewegen, 1990; Moga et al., 1995), which receive inputs from caudal regions of the nucleus of the solitary tract (Ricardo and Koh, 1978) and parabrachial nucleus (Saper and Loewy, 1980).

Inputs from behavior control column—Unlike other BST anterior division components, the BSTam (especially dorsally) receives clear neural inputs from multiple components of the behavior control column, including the lateral part of the medial preoptic nucleus (Simerly and Swanson, 1988), anterior hypothalamic nucleus (Risold et al., 1994), both major parts of the ventromedial hypothalamic nucleus (Canteras et al., 1994), and ventral premammillary nucleus (Canteras et al., 1992). All of these nuclei receive topographically ordered inputs from the medial amygdalar nucleus and BST posterior division (see Dong and Swanson, 2004b), as does the BSTam (see above), and all of them are involved in controlling the expression of social (reproductive and defensive) behaviors (Swanson, 2000).

Inputs from behavioral state control system—Within the BSTam, dopaminergic fibers appear to arise, at least in part, from the ventral tegmental area and caudally adjacent retrorubral areas (Moore, 1978; Hökfelt et al., 1980; Deutch et al., 1988); noradrenergic fibers probably arise at least in part from the locus ceruleus (Jones and Yang, 1985); serotonergic fibers arise from the raphé nuclei (Vertes, 1991; Vertes et al., 1999); histaminergic fibers arise from the tuberomammillary nucleus (Inagaki et al., 1988), hypocretin/orexin fibers arise in or near the lateral hypothalamic area's dorsal region (Allen

and Cechetto, 1993; Peyron et al., 1998); and other fibers arise in the supramammillary (Vertes, 1992) and posterior hypothalamic (Vertes et al., 1995) nuclei.

Comparison of projections from BSTamg components

As with the BST anterolateral group (Dong and Swanson, 2004a), it is useful briefly to compare the major projection patterns established by the various components of the BSTamg (the BST dorsomedial, magnocellular, ventral, and fusiform nuclei, and the BSTam), now that all of them have been described with the PHAL method (Table 1). From Table 1 it is obvious that each BST anteromedial group component establishes a unique projection pattern, although overall they share many broad features in common. As detailed in the preceding paper (Dong and Swanson, 2005a) the projections of the magnocellular nucleus are a subset of those generated by the dorsomedial nucleus, and the projections of the ventral nucleus are a subset of those arising in the magnocellular nucleus. With three potentially important exceptions the projections of the BSTam are a subset of those generated by the dorsomedial nucleus. Exceptionally, the BSTam is the only part of the BST anterior division that innervates significantly the arcuate hypothalamic and mediodorsal thalamic nuclei, and unlike the dorsomedial nucleus it also provides an input to the histaminergic tuberomammillary nucleus. Also unlike the BST dorsomedial nucleus, the BSTam does not significantly innervate orofacial motor-related, humorosensory, thirst-related, and viscerosensory cell groups. The BST fusiform nucleus, which Ju and Swanson (1989) originally included in the anteroventral area (see *Nomenclature*, above), is also a subset of BST dorsomedial nucleus projections except that the fusiform nucleus innervates the parabrachial nucleus—and does not innervate humorosensory, thirst-related nuclei.

There are several obvious differences between projections of the BST anteromedial and anterolateral groups. First, the anteromedial group heavily and directly innervates neuroendocrine components of the hypothalamus whereas the anterolateral group does not. Second, the anteromedial group much more clearly innervates brainstem regions associated with pelvic nerve functions. Third, the anterolateral group innervates much more strikingly hindbrain sensory and motor regions associated with the vagus nerve. And fourth, overall the anterolateral group tends to innervate regions associated with energy balance homeostasis and feeding behavior, whereas the anteromedial group tends to innervate regions (including the subfornical organ and median preoptic nucleus) associated with water balance homeostasis and drinking behavior—as well as with energy balance homeostasis and feeding behavior.

Acknowledgments

ABBREVIATIONS

AAA	anterior amygdalar area
ACB	nucleus accumbens
aco	anterior commissure, olfactory limb
act	anterior commissure, temporal limb
ADP	anterodorsal preoptic nucleus
AHA	anterior hypothalamic area
AHN	anterior hypothalamic nucleus

AHNa	anterior hypothalamic nucleus, anterior part
AHNc	anterior hypothalamic nucleus, central part
AHNd	anterior hypothalamic nucleus, dorsal part
AHNp	anterior hypothalamic nucleus, posterior part
AMBv	nucleus ambiguus, ventral part
Amd	anteromedial nucleus thalamus, dorsal part
Amv	anteromedial nucleus thalamus, ventral part
AOB	accessory olfactory bulb
AONpv	anterior olfactory nucleus, posteroventral part
AQ	cerebral aqueduct
ARH	arcuate nucleus hypothalamus
AVP	anteroventral preoptic nucleus
AVPV	anteroventral periventricular nucleus
B	Barrington's nucleus
BA	bed nucleus accessory olfactory tract
BAC	bed nucleus anterior commissure
BLAa	basolateral nucleus amygdala, anterior part
BLAp	basolateral nucleus amygdala, posterior part
BMA	basomedial nucleus amygdala
BMAa	basomedial nucleus amygdala, anterior part
BMAp	basomedial nucleus amygdala, posterior part
bp	bouton of passage
BST	bed nuclei of the stria terminalis
BSTal	bed nuclei of the stria terminalis, anterior division, anterolateral area
BSTalg	bed nuclei of the stria terminalis, anterior division, anterolateral group
BSTam	bed nuclei of the stria terminalis, anterior division, anteromedial area
BSTamg	bed nuclei of the stria terminalis, anterior division, anteromedial group
BSTd	bed nuclei of the stria terminalis, posterior division, dorsal nucleus
BSTdm	bed nuclei of the stria terminalis, anterior division, dorsomedial nucleus
BSTfu	bed nuclei of the stria terminalis, anterior division, fusiform nucleus
BSTif	bed nuclei of the stria terminalis, posterior division, interfascicular nucleus
BSTju	bed nuclei of the stria terminalis, anterior division, juxtacapsular nucleus
BSTmg	bed nuclei of the stria terminalis, anterior division, magnocellular nucleus
BSTov	bed nuclei of the stria terminalis, anterior division, oval nucleus
BSTp	bed nuclei of the stria terminalis, posterior division
BSTpr	bed nuclei of the stria terminalis, posterior division, principal nucleus

BSTrh	bed nuclei of the stria terminalis, anterior division, rhomboid nucleus
BSTse	bed nuclei of the stria terminalis, posterior division, stria extension
BSTsz	bed nuclei of the stria terminalis, posterior division, cell-sparse zone
BSTtr	bed nuclei of the stria terminalis, posterior division, transverse nucleus
BSTv	bed nuclei of the stria terminalis, anterior division, ventral nucleus
CA1	field CA1, Ammon's horn
CEA	central nucleus amygdala
CEAc	central nucleus amygdala, capsular part
CEAl	central nucleus amygdala, lateral part
CEAm	central nucleus amygdala, medial part
CLI	central linear nucleus raphé
CM	central medial nucleus thalamus
COAa1	2, cortical nucleus amygdala, anterior part, layers 1, 2
COApl1-3	cortical nucleus amygdala, posterior part, lateral zone, layers 1–3
COApm	cortical nucleus amygdala, posterior part, medial zone
COM	commissural nucleus, periaqueductal gray
CP	caudoputamen
cpd	cerebral peduncle
CRH	corticotropin releasing hormone
CSl	superior central nucleus raphé, lateral part
CSm	superior central nucleus raphé, medial part
CUN	cuneiform nucleus
DA	dopamine
DMH	dorsomedial nucleus hypothalamus
DMHa	dorsomedial nucleus hypothalamus, anterior part
DMHp	dorsomedial nucleus hypothalamus, posterior part
DMHv	dorsomedial nucleus hypothalamus, ventral part
DR	dorsal nucleus raphé
dscp	decussation superior cerebellar peduncle
DTN	dorsal tegmental nucleus
ENT	entorhinal area
ENTl1-6	entorhinal area, lateral part, layers 1–6
ENTmv	entorhinal area, medial part, ventral zone
Epv	endopiriform nucleus, ventral part
EW	Edinger-Westphal nucleus
FF	fields of Forel

fi	fimbria
fr	fasciculus retroflexus
FS	fundus of the striatum
fx	columns of the fornix
GPe	globus pallidus, external segment
HF	hippocampal formation
I	internuclear area
IA	intercalated nuclei amygdala
IF	interfascicular nucleus raphé
III	oculomotor nucleus
ILA	infralimbic cortical area
im	internal medullary lamina thalamus
IMD	intermediodorsal nucleus thalamus
INS	insular region
int	internal capsule
IPNr	interpeduncular nucleus, rostral subnucleus
isl	islands of Calleja
Ivn	trochlear nerve
KF	Kölliker-Fuse subnucleus (of PB)
LC	locus ceruleus
LDT	laterodorsal tegmental nucleus
LH	lateral habenula
LHA	lateral hypothalamic area
LHAa	lateral hypothalamic area, anterior region
LHAad	lateral hypothalamic area, anterior region, dorsal zone
LHAai	lateral hypothalamic area, anterior region, intermediate zone
LHAav	lateral hypothalamic area, anterior region, ventral zone
LHAd	lateral hypothalamic area, dorsal region
LHAjd	lateral hypothalamic area, juxtadorsomedial region
LHAjp	lateral hypothalamic area, juxtaparaventricular region
LHAjvd	lateral hypothalamic area, juxtaventromedial region, dorsal zone
LHAjvv	lateral hypothalamic area, juxtaventromedial region, ventral zone
LHAm	lateral hypothalamic area, magnocellular nucleus
LHAp	lateral hypothalamic area, posterior region
LHApc	lateral hypothalamic area, parvicellular region
LHAs	lateral hypothalamic area, suprafornical region

LHAsfa	lateral hypothalamic area, subfornical region, anterior zone
LHAsfp	lateral hypothalamic area, subfornical region, posterior zone
LHAsfpm	lateral hypothalamic area, subfornical region, premammillary zone
LHAvl	lateral hypothalamic area, ventral region, lateral zone
LHAvm	lateral hypothalamic area, ventral region, medial zone
LM	lateral mammillary nucleus
lot	lateral olfactory tract
LPO	lateral preoptic area
LRNm	lateral reticular nucleus, magnocellular part
LS	lateral septal nucleus
LSc	lateral septal nucleus, caudal part
LSr	lateral septal nucleus, rostral part
LSr.m	lateral septal nucleus, rostral part, medial zone
LSr.m.v.c /r	lateral septal nucleus, rostral part, medial zone, ventral region, caudal/ rostral domains
LSr.vl.v	lateral septal nucleus, rostral part, ventrolateral zone, ventral region
LSv	lateral septal nucleus, ventral part
LTN	lateral tegmental nucleus
MA	magnocellular preoptic nucleus
mct	medial corticohypothalamic tract
MDc	mediodorsal nucleus thalamus, central part
MDl	mediodorsal nucleus thalamus, lateral part
MDm	mediodorsal nucleus thalamus, medial part
MDRNv	medullary reticular nucleus, ventral part
ME	median eminence
MEA	medial nucleus amygdala
MEAad	medial nucleus amygdala, anterodorsal part
MEAav	medial nucleus amygdala, anteroventral part
MEApd-a	b,c, medial nucleus amygdala, posterodorsal part, sublayers a-c
MEApv	medial nucleus amygdala, posteroventral part
MEPO	median preoptic nucleus
MEV	midbrain nucleus of the trigeminal
MH	medial habenula
ml	medial lemniscus
mlf	medial longitudinal fascicle
MM	medial mammillary nucleus

MOB	main olfactory bulb
MOC	main olfactory cortex
mp	mammillary peduncle
MPN	medial preoptic nucleus
MPNc	medial preoptic nucleus, central part
MPNl	medial preoptic nucleus, lateral part
MPNm	medial preoptic nucleus, medial part
MPO	medial preoptic area
MRNm	midbrain reticular nucleus, magnocellular part
MRNp	midbrain reticular nucleus, parvicellular part
MS	medial septal nucleus
mtt	mammillothalamic tract
NC	nucleus circularis
ND	nucleus of Darkschewitsch
NDB	nucleus of the diagonal band
NLOT	nucleus of the lateral olfactory tract
NLOT1	nucleus of the lateral olfactory tract, molecular layer
NLOT2	nucleus of the lateral olfactory tract, pyramidal layer
NLOT3	nucleus of the lateral olfactory tract, dorsal cap
NTS	nucleus of the solitary tract
NTSce	nucleus of the solitary tract, central part
NTSco	nucleus of the solitary tract, commissural part
NTSl	nucleus of the solitary tract, lateral part
NTSm	nucleus of the solitary tract, medial part
och	optic chiasm
opt	optic tract
ORBv	orbital area, ventral part
OT	olfactory tubercle
OT1	olfactory tubercle, molecular layer
OT2	olfactory tubercle, pyramidal layer
OT3	olfactory tubercle, polymorph layer
OV	vascular organ lamina terminalis
OXY	oxytocin
PA	posterior nucleus amygdala
PAG	periaqueductal gray
PAGd	periaqueductal gray, dorsal division

PAGdl	periaqueductal gray, dorsolateral division
PAGm	periaqueductal gray, medial division
PAGrm	periaqueductal gray, rostromedial division
PAGvl	periaqueductal gray, ventrolateral division
PARN	parvicellular reticular nucleus
PB	parabrachial nucleus
PBlc	parabrachial nucleus, central lateral part
PBld	parabrachial nucleus, dorsal lateral part
PBle	parabrachial nucleus, external lateral part
PBlv	parabrachial nucleus, ventral lateral part
PBmm	parabrachial nucleus, medial medial part
pc	posterior commissure
PCG	pontine central gray
PH	posterior hypothalamic nucleus
PL	prelimbic cortical area
pm	principal mammillary tract
PMd	dorsal premammillary nucleus
PMv	ventral premammillary nucleus
PP	peripeduncular nucleus
PPN	pedunculopontine nucleus
PR	perireuniens nucleus
PRC	precommissural nucleus, periaqueductal gray
PRNc	pontine reticular nucleus, caudal part
PRNr	pontine reticular nucleus, rostral part
PS	parastrial nucleus
PST	preparasubthalamic nucleus
PSTN	parasubthalamic nucleus of the lateral hypothalamic area
PT	paratenial nucleus
PVa	anterior periventricular nucleus hypothalamus
PVH	paraventricular nucleus hypothalamus
PVHam	paraventricular nucleus hypothalamus, anterior magnocellular part
PVHap	paraventricular nucleus hypothalamus, anterior parvicellular part
PVHd	paraventricular nucleus hypothalamus, descending division
PVHdp	paraventricular nucleus hypothalamus, dorsal parvicellular part
PVHf	paraventricular nucleus hypothalamus, forniceal part
PVHlp	paraventricular nucleus hypothalamus, lateral parvicellular part

PVHmpd	paraventricular nucleus hypothalamus, medial parvicellular part, dorsal zone
PVHmpv	paraventricular nucleus hypothalamus, medial parvicellular part, ventral zone
PVHne	paraventricular nucleus hypothalamus, neuroendocrine division
PVHpml	paraventricular nucleus hypothalamus, posterior magnocellular part, lateral zone
PVHpmm	paraventricular nucleus hypothalamus, posterior magnocellular part, medial zone
PVHpv	paraventricular nucleus hypothalamus, periventricular part
PVi	intermediate periventricular nucleus hypothalamus
PVp	posterior periventricular nucleus hypothalamus
PVpo	preoptic periventricular nucleus
PVT	paraventricular nucleus thalamus
RCH	retrochiasmatic area
RE	nucleus reuniens
REa	nucleus reuniens, rostral division, anterior part
REcd	nucleus reuniens, caudal division, dorsal part
REcm	nucleus reuniens, caudal division, median part
REcp	nucleus reuniens, caudal division, posterior part
REd	nucleus reuniens, rostral division, dorsal part
REl	nucleus reuniens, rostral division, lateral part
REm	nucleus reuniens, rostral division, medial part
REv	nucleus reuniens, rostral division, ventral part
RL	rostral linear nucleus raphé
RM	nucleus raphé magnus
RN	red nucleus
RR	midbrain reticular nucleus, retrorubral area
RT	reticular nucleus thalamus
rust	rubrospinal tract
SBPV	subparaventricular zone hypothalamus
SCH	suprachiasmatic nucleus
scp	superior cerebellar peduncle
sctv	ventral spinocerebellar tract
SF	septofimbrial nucleus
SI	substantia innominata
SLD	sublaterodorsal nucleus

sm	stria medullaris
smd	supramammillary decussation
SMT	submedial nucleus thalamus
SNc	substantia nigra, compact part
SO	supraoptic nucleus
SOr	supraoptic nucleus, retrochiasmatic part
SS	somatostatin
st	stria terminalis
STN	subthalamic nucleus
SUBv	subiculum, ventral part
SUMl	supramammillary nucleus, lateral part
SUMm	supramammillary nucleus, medial part
sup	supraoptic commissures
SUT	supratrigeminal nucleus
tb	terminal bouton
TEa	temporal association areas
TMd	tuberomammillary nucleus, dorsal part
TMv	tuberomammillary nucleus, ventral part
TR1-3	postpiriform transition area, layers 1–3
TRH	thyrotropin releasing hormone
ts	solitary tract
tsp	tectospinal pathway
TTd/v	tenia tecta, dorsal/ventral parts
TU	tuberal nucleus
TUi	tuberal nucleus, intermediate part
TUl	tuberal nucleus, lateral part
TUsv	tuberal nucleus, subventromedial part
TUte	tuberal nucleus, terete subnucleus
v	varicosity
V3	third ventricle
V3M	third ventricle, mammillary recess
V3p	third ventricle, preoptic recess
V4	fourth ventricle
VL	lateral ventricle
vlt	ventrolateral hypothalamic tract
Vma	motor nucleus of the trigeminal, magnocellular part

VMH	ventromedial nucleus hypothalamus
VMHa	ventromedial nucleus hypothalamus, anterior part
VMHc	ventromedial nucleus hypothalamus, central part
VMHdm	ventromedial nucleus hypothalamus, dorsomedial part
VMHvl	ventromedial nucleus hypothalamus, ventrolateral part
Vpc	motor nucleus of the trigeminal, parvicellular part
VTA	ventral tegmental area
vtd	ventral tegmental decussation
XII	hypoglossal nucleus
ZI	zona incerta
ZIda	zona incerta, dopaminergic group
zl	zona limitans

LITERATURE CITED

Alden M, Besson JM, Bernard JF. Organization of the efferent projections from the pontine parabrachial area to the bed nucleus of the stria terminalis and neighboring regions: a PHA-L study in the rat. J Comp Neurol. 1994; 341:289–314. [PubMed: 7515078]

Allen GV, Cechetto DF. Functional and anatomical organization of cardiovascular pressor and depressor sites in the lateral hypothalamic area. II. Ascending projections. J Comp Neurol. 1993; 330:421–438. [PubMed: 7682225]

Alvarez-Bolado, G.; Swanson, LW. Developmental brain maps: structure of the embryonic rat brain. Amsterdam: Elsevier; 1996.

Bayer SA. Neurogenetic and morphogenetic heterogeneity in the bed nucleus of the stria terminalis. J Comp Neurol. 1987; 265:47–64. [PubMed: 3693604]

Berendse HW, Groenewegen HJ. Organization of the thalamostriatal projections in the rat, with special emphasis on the ventral striatum. J Comp Neurol. 1990; 299:187–228. [PubMed: 2172326]

Berendse HW, Groenewegen HJ, Lohman AH. Compartmental distribution of ventral striatal neurons projecting to the mesencephalon in the rat. J Neurosci. 1992; 12:2079–2103. [PubMed: 1607929]

Brog JS, Salyapongse A, Deutch AY, Zahm DS. The patterns of afferent innervation of the core and shell in the "accumbens" part of the rat ventral striatum: immunohistochemical detection of retrogradely transported fluorogold. J Comp Neurol. 1993; 338:255–278. [PubMed: 8308171]

Canteras NS, Simerly RB, Swanson LW. Projections of the ventral premammillary nucleus. J Comp Neurol. 1992; 324:195–212. [PubMed: 1430329]

Canteras NS, Simerly RB, Swanson LW. Organization of the ventromedial nucleus of the hypothalamus: a phaseolus vulgaris-leucoagglutinin study in the rat. J Comp Neurol. 1994; 348:41–79. [PubMed: 7814684]

Canteras NS, Swanson LW. Projection of the ventral subiculum to the amygdala, septum and hypothalamus: a PHAL anterograde tract-tracing study in the rat. J Comp Neurol. 1992; 324:180–194. [PubMed: 1430328]

Cassell MD, Freedman LJ, Shi C-J. The intrinsic organization of the central extended amygdala. Ann NY Acad Sci. 1999; 877:217–241. [PubMed: 10415652]

Chen S, Su HS. Afferent connections of the thalamic paraventricular and parataenial nuclei in the rat—a retrograde tracing study with iontophoretic application of Fluoro-Gold. Brain Res. 1990; 522:1–6. [PubMed: 2224500]

Ciccocioppo R, Fedeli A, Economidou D, Policani F, Weiss F, Massi M. The bed nucleus is a neuroanatomical substrate for the anorectic effect of corticotropin-releasing factor and for its reversal by nociceptin/orphanin FQ. J Neurosci. 2003; 23:9445–9451. [PubMed: 14561874]

Cullinan WE, Herman JP, Watson SJ. Ventral subicular interaction with the hypothalamic paraventricular nucleus: evidence for a relay in the bed nucleus of the stria terminalis. J Comp Neurol. 1993; 332:1–20. [PubMed: 7685778]

de Olmos JS, Ingram WR. The projection field of the stria terminalis in the rat brain. An experimental study. J Comp Neurol. 1972; 146:303–334. [PubMed: 5086675]

Deutch AY, Goldstein M, Baldino F Jr, Roth RH. Telencephalic projections of the A8 dopamine cell group. Ann NY Acad Sci. 1988; 537:27–50. [PubMed: 2462395]

Dong H-W, Petrovich GD, Swanson LW. Organization of projections from the juxtacapsular nucleus of the BST: a PHAL study in the rat. Brain Res. 2000; 859:1–14. [PubMed: 10720609]

Dong H-W, Petrovich GD, Swanson LW. Topography of projections from amygdala to bed nuclei of the stria terminalis. Brain Res Rev. 2001a; 38:192–246. [PubMed: 11750933]

Dong H-W, Petrovich GD, Watts AG, Swanson LW. Basic organization of projections from the oval and fusiform nuclei of the bed nuclei of the stria terminalis in adult rat brain. J Comp Neurol. 2001b; 436:430–455. [PubMed: 11447588]

Dong H-W, Swanson LW. Projections from the rhomboid nucleus of the bed nuclei of the stria terminalis: implications for cerebral hemisphere regulation of ingestive behaviors. J Comp Neurol. 2003; 463:434–472. [PubMed: 12836178]

Dong H-W, Swanson LW. Organization of axonal projections from the anterolateral area of the bed nuclei of the stria terminalis. J Comp Neurol. 2004a; 468:277–298. [PubMed: 14648685]

Dong H-W, Swanson LW. Projections from bed nuclei of the stria terminalis, posterior division: implications for cerebral hemisphere regulation of defensive and reproductive behaviors. J Comp Neurol. 2004b; 471:396–433. [PubMed: 15022261]

Dong H-W, Swanson LW. Axonal projections from bed nuclei of the stria terminalis, dorsomedial nucleus: implications for cerebral hemisphere regulation of autonomic, neuroendocrine, and drinking responses. J Comp Neurol. 2005a (in press).

Dong H-W, Swanson LW. Projections from the bed nuclei of the stria terminalis, magnocellular nucleus: implications for cerebral hemisphere regulation of micturition, defecation, and penile erection. J Comp Neurol. 2005b (in press).

Elmquist JK, Elias CF, Saper CB. From lesions to leptin: hypothalamic control of food intake and body weight. Neuron. 1999; 22:221–232. [PubMed: 10069329]

Gerfen CR, Sawchenko PE. An anterograde neuroanatomical tracing method that shows the detailed morphology of neurons, their axons and terminals: immunohistochemical localization of an axonally transported plant lectin, *Phaseolus vulgaris*-leucoagglutinin (PHA-L). Brain Res. 1984; 290:219–238. [PubMed: 6198041]

Gonzalo-Ruiz A, Alonso A, Sanz JM, Llinas RR. Afferent projections to the mammillary complex of the rat, with special reference to those from surrounding hypothalamic regions. J Comp Neurol. 1992; 321:277–299. [PubMed: 1380015]

Gray TS, Magnuson DJ. Peptide immunoreactive neurons in the amygdala and the bed nucleus of the stria terminalis project to the midbrain central gray in the rat. Peptides. 1992; 13:451–460. [PubMed: 1381826]

Groenewegen HJ. Organization of the afferent connections of the mediodorsal thalamic nucleus in the rat, related to the mediodorsal-prefrontal topography. Neurosci. 1988; 24:379–431.

Groenewegen HJ, Russchen FT. Organization of the efferent projections of the nucleus accumbens to pallidal, hypothalamic, and mesencephalic structures: a tracing and immunohistochemical study in the cat. J Comp Neurol. 1984; 223:347–367. [PubMed: 6323552]

Grove EA. Neural associations of the substantia innominata in the rat: afferent connections. J Comp Neurol. 1988; 277:315–346. [PubMed: 2461972]

Gu GB, Cornea A, Simerly RB. Sexual differentiation of projections from the principal nuclei of the bed nuclei of the stria terminalis. J Comp Neurol. 2003; 460:542–562. [PubMed: 12717713]

Herbert H, Moga MM, Saper CB. Connections of the parabrachial nucleus with the nucleus of the solitary tract and the medullary reticular formation in the rat. J Comp Neurol. 1990; 293:540–580. [PubMed: 1691748]

Herman JP, Cullinan WE. Neurocircuitry of stress: central control of the hypothalamo-pituitary-adrenocortical axis. Trends Neurosci. 1997; 20:78–84. [PubMed: 9023876]

Herman JP, Tasker JG, Ziegler DR, Cullinan WE. Local circuit regulation of paraventricular nucleus stress integration: glutamate-GABA connections. Pharmacol Biochem Behav. 2002; 71:457–468. [PubMed: 11830180]

Hökfelt T, Skirboll L, Rehfeld JF, Goldstein M, Markey K, Dann O. A subpopulation of mesencephalic dopamine neurons projecting to limbic areas contains a cholecystokinin-like peptide: evidence from immunohistochemistry combined with retrograde tracing. Neurosci. 1980; 5:2093–2124.

Hurley KM, Herbert H, Moga MM, Saper CB. Efferent projections of the infralimbic cortex of the rat. J Comp Neurol. 1991; 308:249–276. [PubMed: 1716270]

Inagaki N, Yamatodani A, Ando-Yamamoto M, Tohyama M, Watanabe T, Wada H. Organization of histaminergic fibers in the rat brain. J Comp Neurol. 1988; 273:283–300. [PubMed: 3062046]

Johnston JB. Further contributions to the study of the evolution of the forebrain. J Comp Neurol. 1923; 35:337–481.

Jones BE, Yang TZ. The efferent projections from the reticular formation and the locus coeruleus studied by anterograde and retrograde axonal transport in the rat. J Comp Neurol. 1985; 242:56–92. [PubMed: 2416786]

Ju G, Swanson LW. Studies on the cellular architecture of the bed nuclei of the stria terminalis in the rat: I. Cytoarchitecture. J Comp Neurol. 1989; 280:587–602. [PubMed: 2708568]

Ju G, Swanson LW, Simerly RB. Studies on the cellular architecture of the bed nuclei of the stria terminalis in the rat: II. Chemoarchitecture. J Comp Neurol. 1989; 280:603–621. [PubMed: 2468695]

Köhler C, Swanson LW, Haglund L, Wu JY. The cytoarchitecture, histochemistry and projections of the tuberomammillary nucleus in the rat. Neurosci. 1985; 16:85–110.

Krettek JE, Price JL. Amygdaloid projections to subcortical structures within the basal forebrain and brainstem in the rat and cat. J Comp Neurol. 1978; 178:225–254. [PubMed: 627625]

Li YQ, Takada M, Shinonaga Y, Mizuno N. The sites of origin of dopaminergic afferent fibers to the lateral habenular nucleus in the rat. J Comp Neurol. 1993; 333:118–133. [PubMed: 8101849]

Markakis EA, Swanson LW. Spatiotemporal patterns of secretomotor neuron generation in the parvicellular neuroendocrine system. Brain Res Rev. 1997; 24:255–291. [PubMed: 9385456]

McDonald AJ. Cortical pathways to the mammalian amygdala. Prog Neurobiol. 1998; 55:257–332. [PubMed: 9643556]

Moga MM, Saper CB. Neuropeptide-immunoreactive neurons projecting to the paraventricular hypothalamic nucleus in the rat. J Comp Neurol. 1994; 346:137–150. [PubMed: 7962708]

Moga MM, Weis RP, Moore RY. Efferent projections of the paraventricular thalamic nucleus in the rat. J Comp Neurol. 1995; 359:221–238. [PubMed: 7499526]

Moore RY. Catecholamine innervation of the basal forebrain. I. The septal area. J Comp Neurol. 1978; 177:665–684. [PubMed: 75215]

Petrovich GD, Swanson LW. Projections from the lateral part of the central amygdalar nucleus to the postulated fear conditioning circuit. Brain Res. 1997; 763:247–254. [PubMed: 9296566]

Peyron C, Tighe DK, van den Pol AN, de Lecea L, Heller HC, Sutcliffe JG, Kilduff TS. Neurons containing hypocretin (orexin) project to multiple neuronal systems. J Neurosci. 1998; 18:9996–10015. [PubMed: 9822755]

Phillipson OT. Afferent projections to the ventral tegmental area of Tsai and interfascicular nucleus: a horseradish peroxidase study in the rat. J Comp Neurol. 1979; 187:117–143. [PubMed: 489776]

Prewitt CM, Herman JP. Anatomical interactions between the central amygdaloid nucleus and the hypothalamic paraventricular nucleus of the rat: a dual tract-tracing analysis. J Chem Neuroanat. 1998; 15:173–185. [PubMed: 9797074]

Ribeiro-Barbosa ER, Skorupa AL, Cipolla-Neto J, Canteras NS. Projections of the basal retrochiasmatic area: a neural site involved in the photic control of pineal metabolism. Brain Res. 1999; 839:35–40. [PubMed: 10482796]

Ricardo JA, Koh ET. Anatomical evidence of direct projections from the nucleus of the solitary tract to the hypothalamus, amygdala, and other forebrain structures in the rat. Brain Res. 1978; 153:1–26. [PubMed: 679038]

Risold PY, Canteras NS, Swanson LW. Organization of projections from the anterior hypothalamic nucleus: a phaseolus vulgaris-leucoagglutinin study in the rat. J Comp Neurol. 1994; 348:1–40. [PubMed: 7814679]

Risold PY, Swanson LW. Connections of the rat lateral septal complex. Brain Res Rev. 1997; 24:115–195. [PubMed: 9385454]

Risold PY, Thompson RH, Swanson LW. The structural organization of connections between hypothalamus and cerebral cortex. Brain Res Rev. 1997; 24:197–154. [PubMed: 9385455]

Roland BL, Sawchenko PE. Local origins of some GABAergic projections to the paraventricular and supraoptic nuclei of the hypothalamus in the rat. J Comp Neurol. 1993; 332:123–143. [PubMed: 7685780]

Saper CB, Loewy AD. Efferent connections of the parabrachial nucleus in the rat. Brain Res. 1980; 197:291–317. [PubMed: 7407557]

Saper CB, Loewy AD, Swanson LW, Cowan WM. Direct hypothalamo-autonomic connections. Brain Res. 1976; 117:305–312. [PubMed: 62600]

Satoh K, Fibiger HC. Cholinergic neurons of the laterodorsal tegmental nucleus: efferent and afferent connections. J Comp Neurol. 1986; 253:277–302. [PubMed: 2432101]

Sawchenko PE. Toward a new neurobiology of energy balance, appetite, and obesity: the anatomists weigh in. J Comp Neurol. 1998; 402:435–441. [PubMed: 9862319]

Sawchenko PE, Swanson LW. The organization of forebrain afferents to the paraventricular and supraoptic nuclei of the rat. J Comp Neurol. 1983; 218:121–144. [PubMed: 6886068]

Sawchenko PE, Swanson LW, Rivier J, Vale WW. The distribution of growth-hormone-releasing factor (GRF) immunoreactivity in the central nervous system of the rat: an immunohistochemical study using antisera directed against rat hypothalamic GRF. J Comp Neurol. 1985; 237:100–115. [PubMed: 3930577]

Schwartz MW, Woods SC, Porte D Jr, Seeley RJ, Baskin DG. Central nervous system control of food intake. Nature. 2000; 404:661–671. [PubMed: 10766253]

Simerly RB, Swanson LW. The organization of neural inputs to the medial preoptic nucleus of the rat. J Comp Neurol. 1986; 246:312–342. [PubMed: 3517086]

Simerly RB, Swanson LW. Projections of the medial preoptic nucleus: a phaseolus vulgaris leucoagglutinin anterograde tract-tracing study in the rat. J Comp Neurol. 1988; 270:209–242. [PubMed: 3259955]

Spencer SJ, Buller KM, Day TA. Medial prefrontal cortex control of the paraventricular hypothalamic nucleus response to psychological stress: possible role of the bed nucleus of the stria terminalis. J Comp Neurol. 2005; 481:363–376. [PubMed: 15593338]

Stratford TR, Kelley AE. GABA in the nucleus accumbens shell participates in the central regulation of feeding behavior. J Neurosci. 1997; 17:4434–4440. [PubMed: 9151760]

Stratford TR, Kelley AE. Evidence of a functional relationship between the nucleus accumbens shell and lateral hypothalamus subserving the control of feeding behavior. J Neurosci. 1999; 19:11040–11048. [PubMed: 10594084]

Sun N, Roberts L, Cassell MD. Rat central amygdaloid nucleus projections to the bed nucleus of the stria terminalis. Brain Res Bull. 1991; 27:651–662. [PubMed: 1721859]

Swanson, LW. Organization of mammalian neuroendocrine system. In: Bloom, FE., editor. Handbook of physiology, the nervous system, IV. Baltimore: Waverly Press; 1986. p. 317-363.

Swanson, LW. Brain maps: structure of the rat brain. 2. Amsterdam: Elsevier; 1998–1999.

Swanson LW. Cerebral hemisphere regulation of motivated behavior. Brain Res. 2000; 886:113–164. [PubMed: 11119693]

Swanson LW. The amygdala and its place in the cerebral hemisphere. Ann NY Acad Sci. 2003; 985:174–184. [PubMed: 12724158]

Swanson, LW. Brain maps: structure of the rat brain. 3. Amsterdam: Elsevier; 2004.

Swanson LW, Cowan WM. An autoradiographic study of the organization of the efferent connections of the hippocampal formation in the rat. J Comp Neurol. 1977; 172:49–84. [PubMed: 65364]

Swanson LW, Cowan WM. The connections of the septal region in the rat. J Comp Neurol. 1979; 186:621–656. [PubMed: 15116692]

Swanson LW, Kuypers HG. The paraventricular nucleus of the hypothalamus: cytoarchitectonic subdivisions and organization of projections to the pituitary, dorsal vagal complex, and spinal cord as demonstrated by retrograde fluorescence double-labeling methods. J Comp Neurol. 1980; 194:555–570. [PubMed: 7451682]

Swanson LW, McKellar S. The distribution of oxytocin- and neurophysin-stained fibers in the spinal cord of the rat and monkey. J Comp Neurol. 1979; 188:87–106. [PubMed: 115910]

Takatsu Y, Matsumoto H, Ohtaki T, Kumano S, Kitada C, Onda H, Nishimura O, Fujino M. Distribution of galanin-like peptide in the rat brain. Endocrinol. 2001; 142:1626–1634.

Thompson RH, Swanson LW. Organization of inputs to the dorsomedial nucleus of the hypothalamus: a reexamination with fluorogold and PHAL in the rat. Brain Res Rev. 1998; 27:89–118. [PubMed: 9622601]

Thompson RH, Swanson LW. Structural characterization of a hypothalamic visceromotor pattern generator network. Brain Res Rev. 2003; 41:153–202. [PubMed: 12663080]

Vertes RP. A PHA-L analysis of ascending projections of the dorsal raphe nucleus in the rat. J Comp Neurol. 1991; 313:643–668. [PubMed: 1783685]

Vertes RP. PHA-L analysis of projections from the supramammillary nucleus in the rat. J Comp Neurol. 1992; 326:595–622. [PubMed: 1484125]

Vertes RP, Crane AM, Colom LV, Bland BH. Ascending projections of the posterior nucleus of the hypothalamus: PHA-L analysis in the rat. J Comp Neurol. 1995; 359:90–116. [PubMed: 8557849]

Vertes RP, Fortin WJ, Crane AM. Projections of the median raphe nucleus in the rat. J Comp Neurol. 1999; 407:555–582. [PubMed: 10235645]

Vertes RP, Kocsis B. Brainstem-diencephalo-septohippocampal systems controlling the theta rhythm of the hippocampus. Neuroscience. 1997; 81:893–926. [PubMed: 9330355]

Watts AG. Neuropeptides and the integration of motor responses to dehydration. Ann Rev Neurosci. 2001; 24:357–384. [PubMed: 11283315]

Weller KL, Smith DA. Afferent connections to the bed nucleus of the stria terminalis. Brain Res. 1982; 232:255–270. [PubMed: 7188024]

Zaborszky L. Afferent connections of the medial basal hypothalamus. Adv Anat Embryol Cell Biol. 1982; 69:1–107. [PubMed: 6277162]
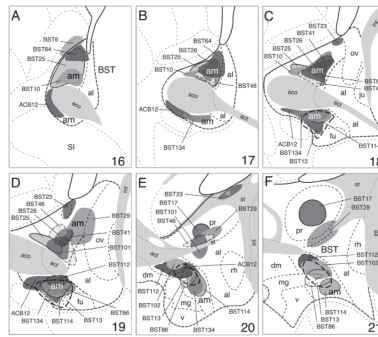
Fig. 1.
Schematic overview of PHAL injection sites involving dorsal and ventral regions of the
BSTam as viewed on six consecutive levels (indicated in the lower right) of the Swanson
atlas (2004); drawings of transverse sections through the right side of the adult male rat
brain are arranged from rostral (A) to caudal (F). Note that together these 18 experiments
label neurons in almost all regions of the BSTam. The exact distribution of labeled neurons
in each experiment is shown in Figure 3. The border of the BST as a whole is indicated by a
thicker dashed line.
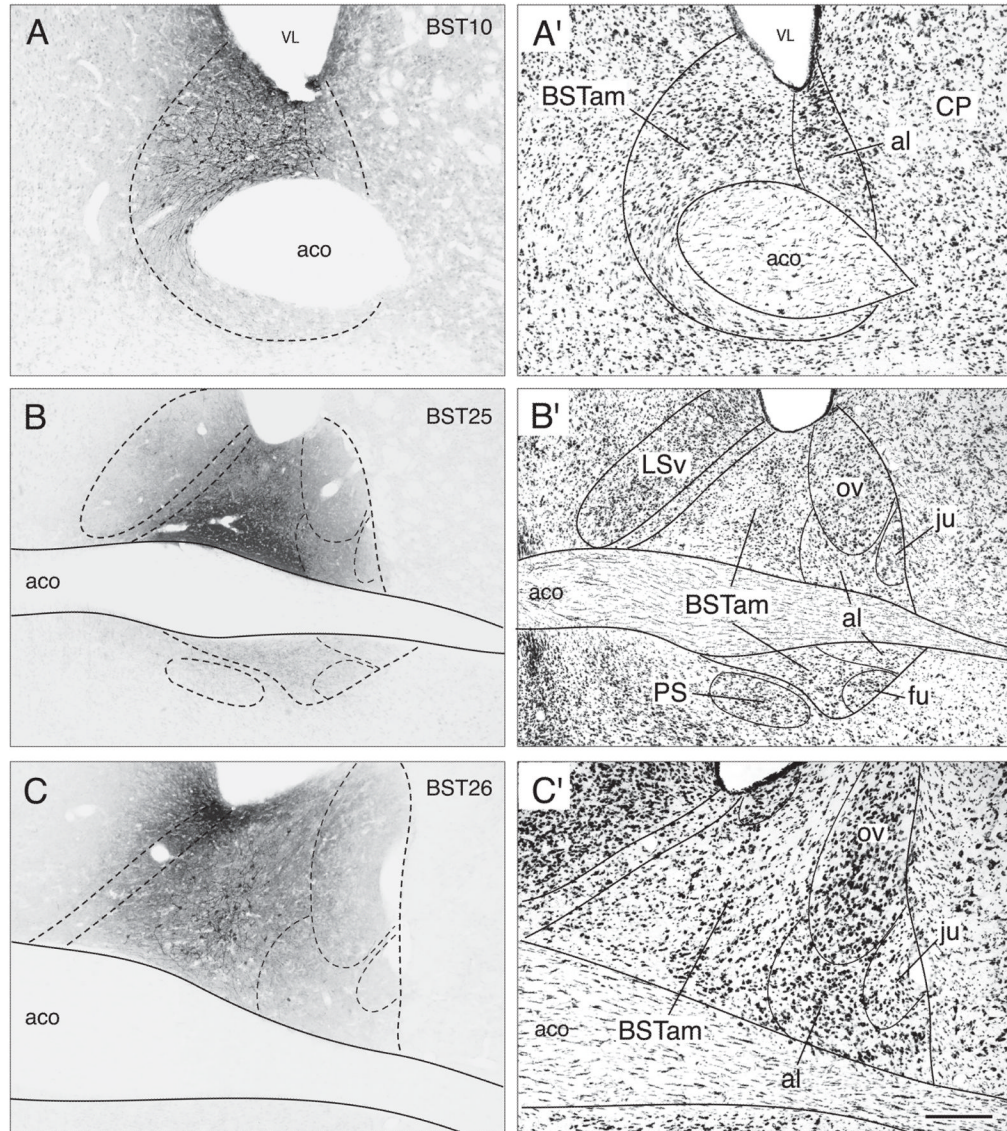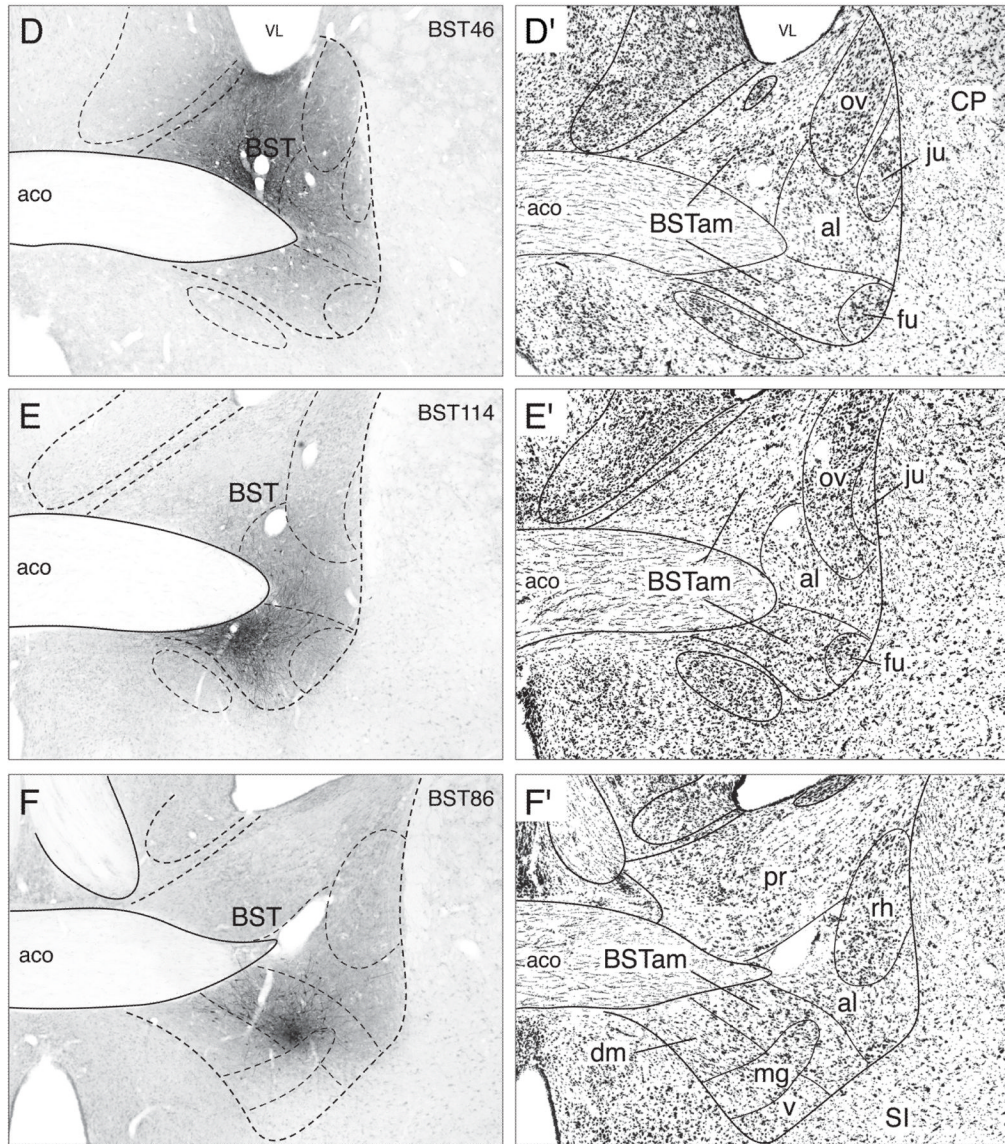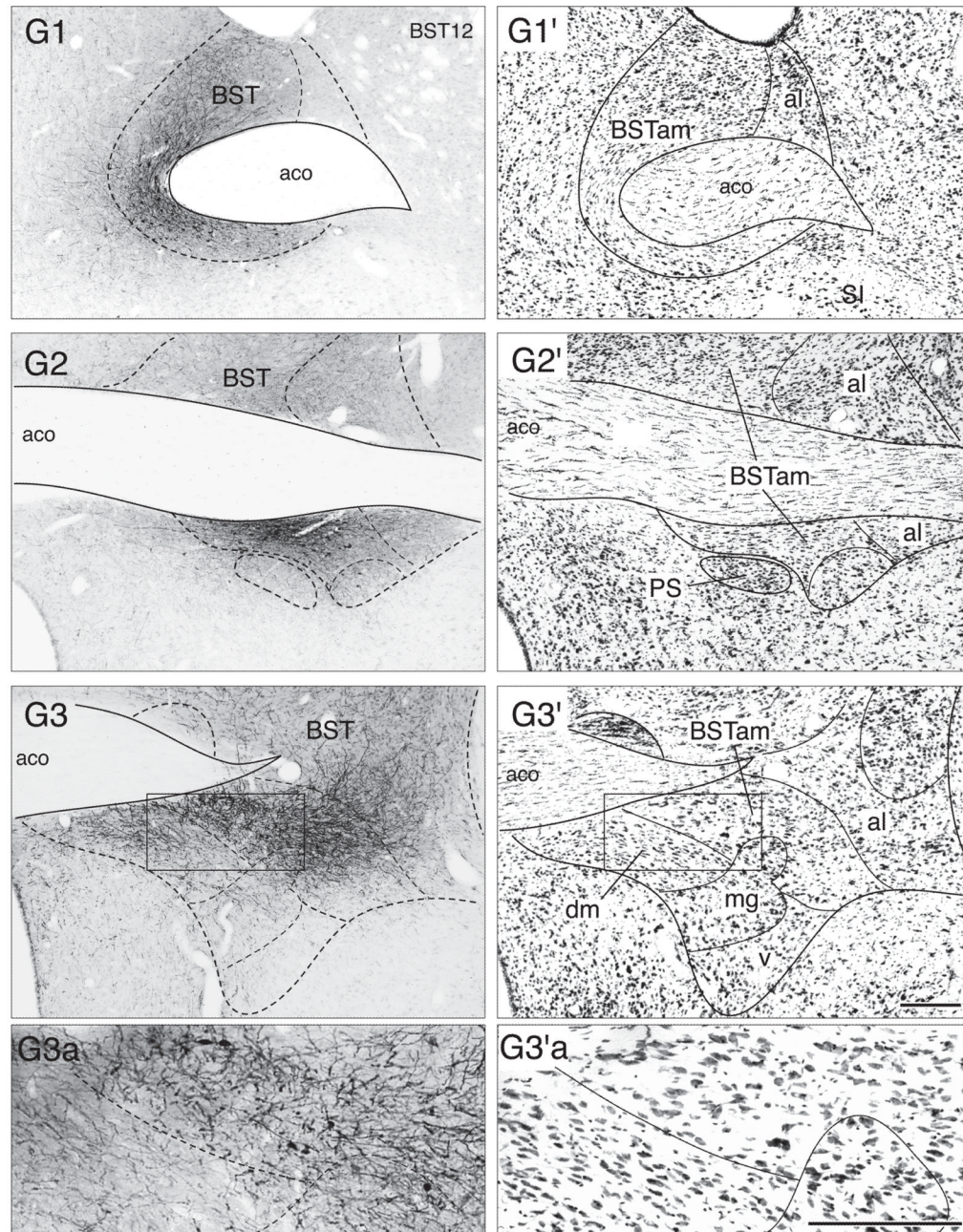
Fig. 2.
Brightfield photomicrographs to show the appearance of a PHAL injection site centered in the rostral region (A, experiment BST10), central core (B, experiment BST25), and caudal region (C, experiment BST26; and D, experiment BST46) of the dorsal BSTam; and a PHAL injection site centered in various rostrocaudal regions of the ventral BSTam (E, experiment BST114; F, experiment BST86; and G, experiment ACB12). The PHAL injection in experiment BST25 involves the greatest extent of the dorsal BSTam (see Fig. 3 for camera lucida drawings of PHAL-labeled neurons), whereas the PHAL injection in experiment ACB12 involves the greatest extent of the ventral BSTam. G1, G2, and G3 show three representative rostrocaudal levels of the PHAL injection in experiment ACB12. Note that PHAL-labeled dendrites of ventral BSTam neurons tend to remain within the area itself,

and do not extend into adjacent regions of the BST dorsomedial nucleus (G3). G3a shows at higher magnification the boxed area in G3. For cytoarchitectonic comparisons an adjacent Nissl-stained section is shown to the right of each PHAL photomicrograph (A′ to G3′a). Different features of these injection sites are illustrated in Figures 1 and 3. All scale bars = 200 μm.
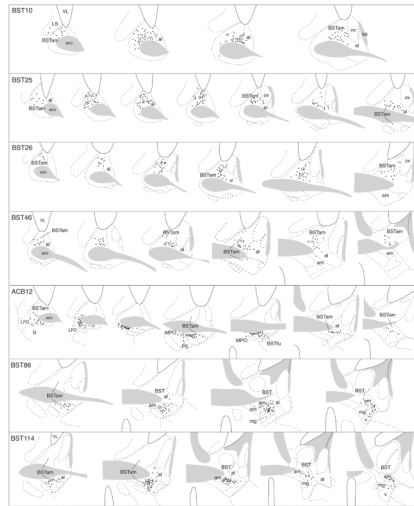
Fig. 3.
Camera lucida plots to show the distribution of PHAL-labeled neurons (black dots) in the BST of transverse histological sections through the injections site in experiments illustrated in Figures 1 and 2. In each row, drawings are arranged from rostral (left) to caudal (right).
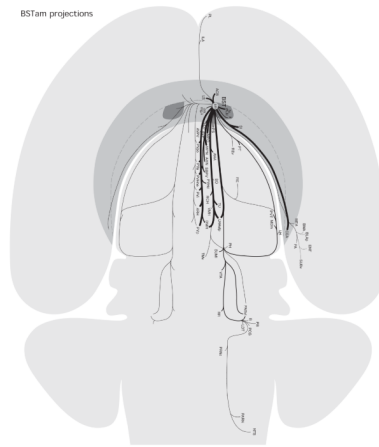
Fig. 4.
This diagram indicates the general organization of projections from the BSTam. The relative strength of each pathway is roughly proportional to the thickness of the line representing it. "BSTam" refers to the overall projection pattern of dorsal as well as ventral regions of the BSTam, which are shown to be indistinguishable with the methods used here. The flatmap is based on Swanson (2004).
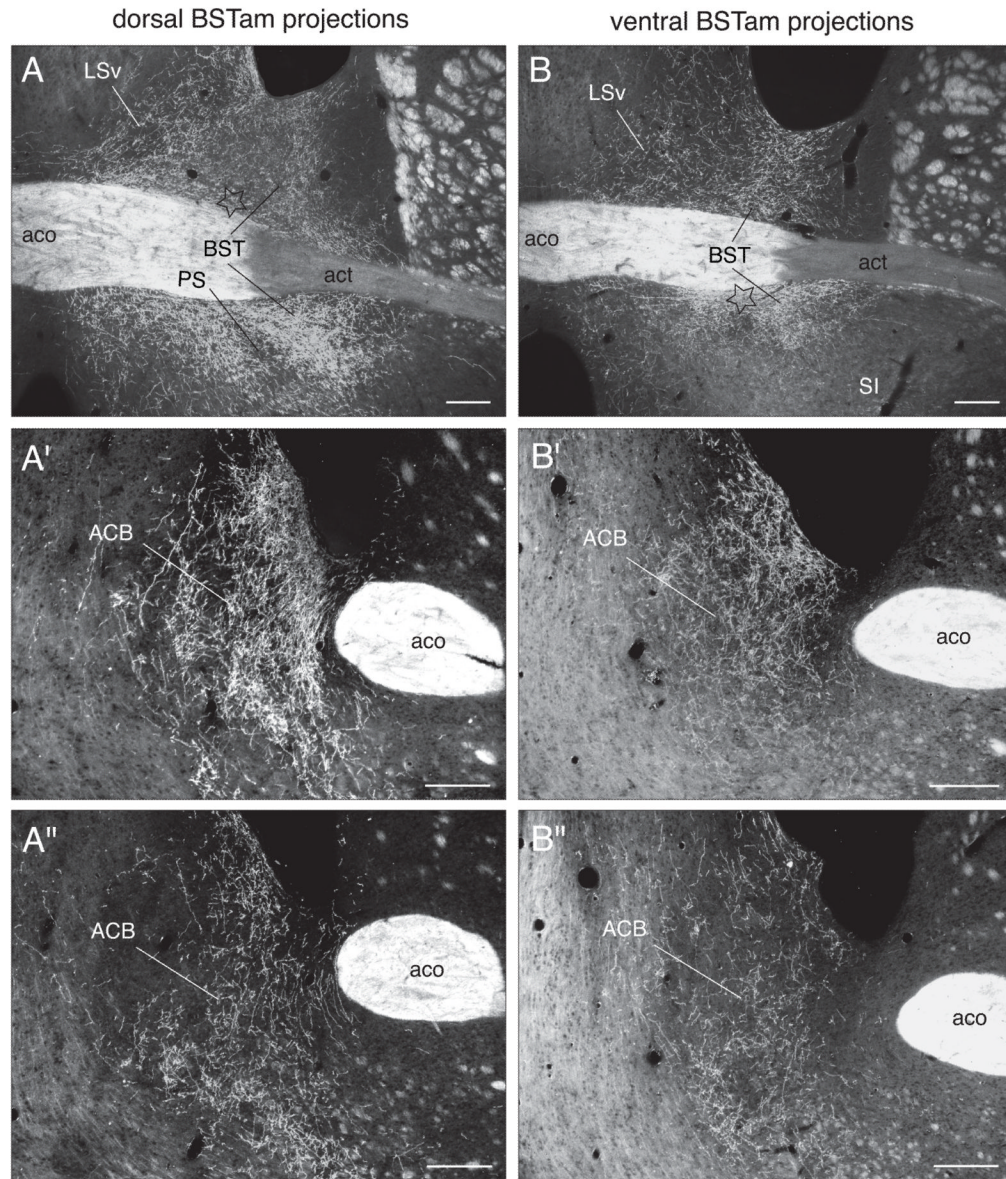
Fig. 5.
Photomicrographs (darkfield illumination) comparing the distribution of PHAL-labeled axons in experiment BST25, where the PHAL injection involves the most extensive region of the dorsal BSTam (A–A″), and in experiment ACB 12, where the PHAL injection involves the most extensive region of the ventral BSTam (B–B″). Micrographs A,B are at a level roughly through the center of the BSTam, and the ventral part of the lateral septal nucleus (approximately level G in Fig. 9); micrographs A′,B′ are at the level of the nucleus accumbens's caudal tip (see level D in Fig. 9); and the micrographs in A″,B″ are somewhat more rostral to A′,B′, illustrating clearly PHAL labeling in medial (shell) regions of the nucleus accumbens (about level C in Fig. 9). Black star in A and B indicates center of injection site. All scale bars = 200 μm.
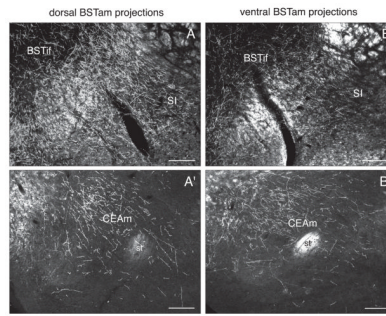
Fig. 6.
Photomicrographs (darkfield illumination) comparing the distribution of PHAL-labeled axons in caudodorsal regions of the substantia innominata (A,B; about level K in Fig. 9) and central amygdalar nucleus (A′,B′; about level P in Fig. 9), following PHAL injections involving either the dorsal BSTam (experiment BST25, A, A′) or the ventral BSTam (experiment ACB12, B, B′). Transverse sections; all scale bars = 200 μm.

dorsal BSTam projections   ventral BSTam projections

dorsal BSTam projections

ventral BSTam projections
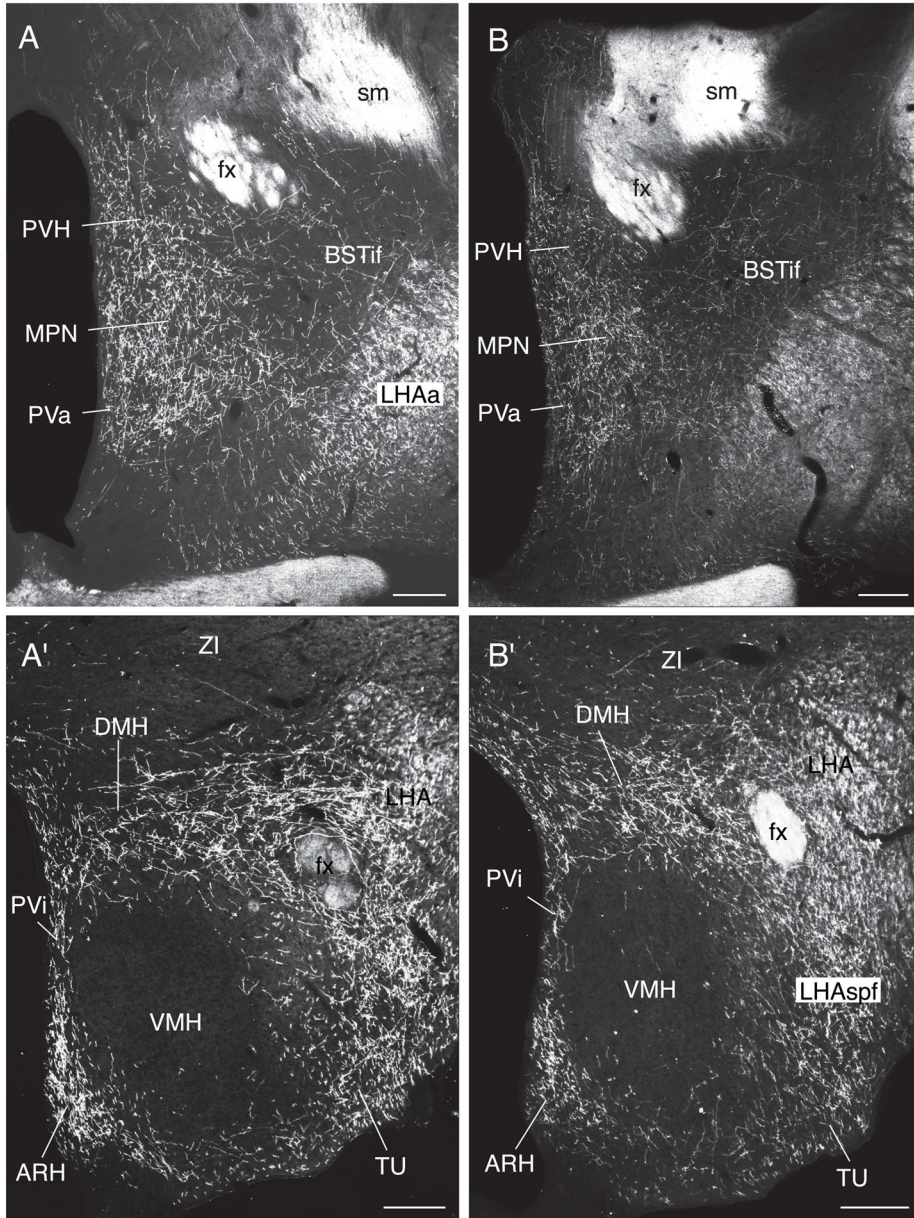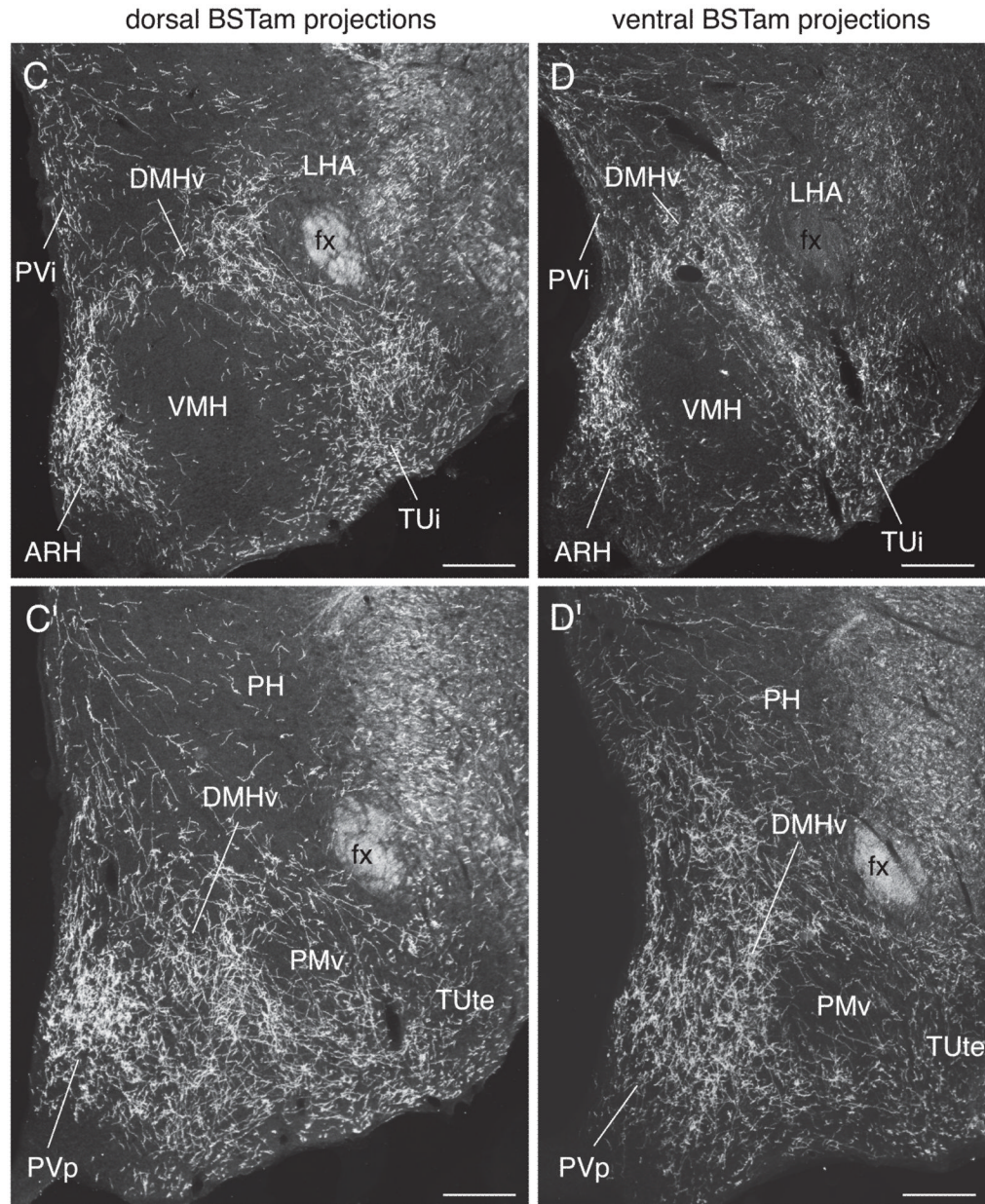
Fig. 7.
Photomicrographs (darkfield illumination) comparing the distribution of PHAL-labeled axons from injections involving the dorsal BSTam (experiment BST25, A, A′, C, C′) or the ventral BSTam (experiment ACB12, B, B′, D, D′)—at the level of the caudal end of the medial preoptic nucleus (A, B; see Fig. 9K), and at three progressively more caudal levels of the dorsomedial hypothalamic nucleus (A′,B′, C,D, C′,D′; see Fig. 9Q,S,T, respectively). Transverse sections; all scale bars = 200 μm.
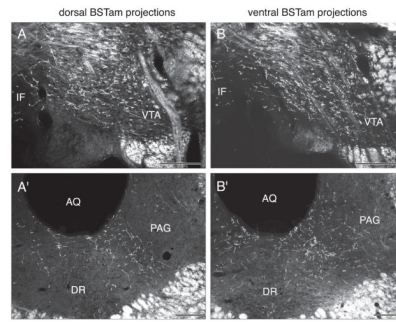
Fig. 8.
Photomicrographs (darkfield illumination) comparing the distribution of PHAL-labeled axons in the ventral tegmental area (A, B; about level Y in Fig. 9) and ventrolateral division of the periaqueductal gray (A′, B′; about level AA in Fig. 9), from PHAL injections involving the dorsal BSTam (experiment BST25, A, A′) or ventral BSTam (experiment ACB12, B, B′). Transverse sections; all scale bars = 200 μm.
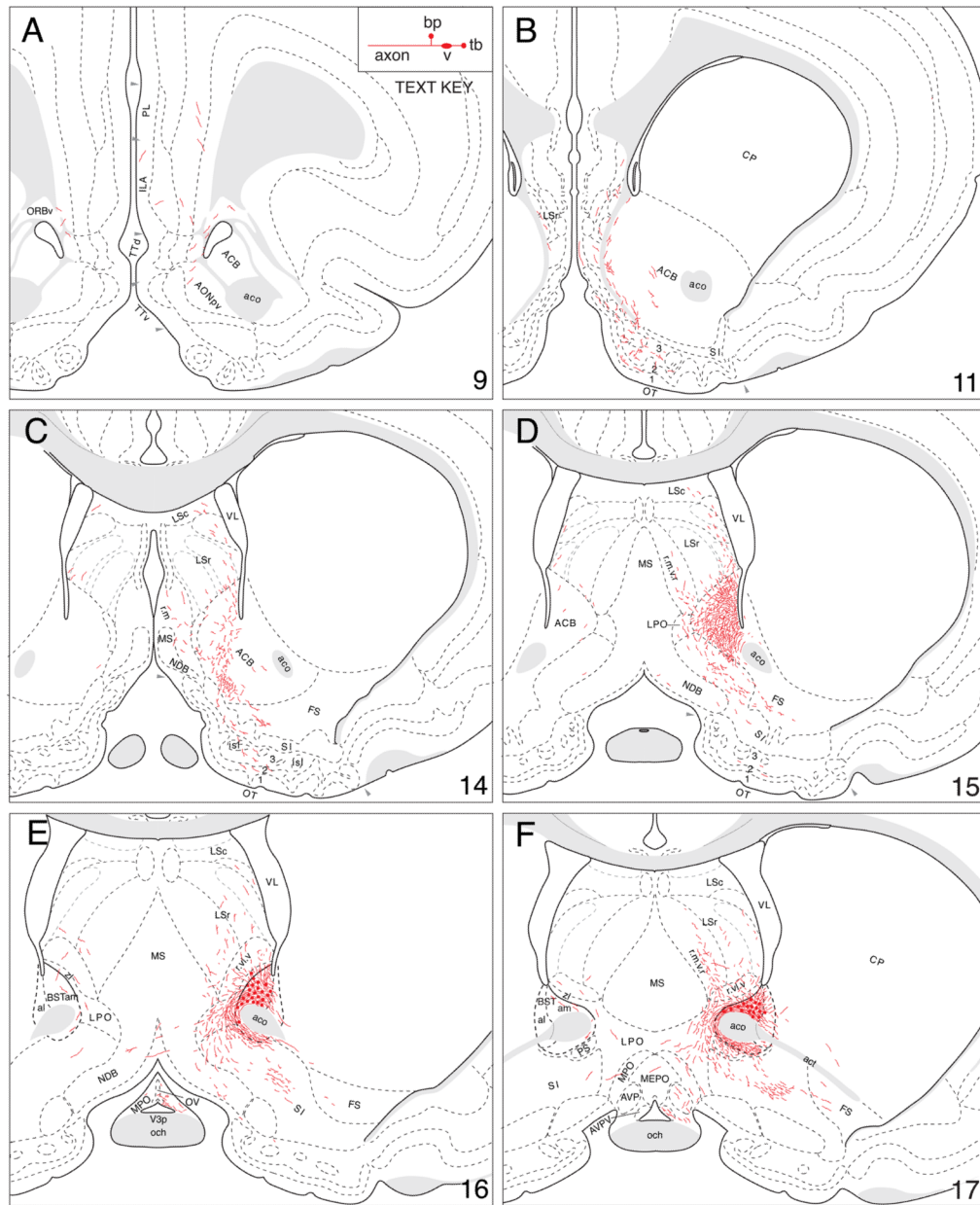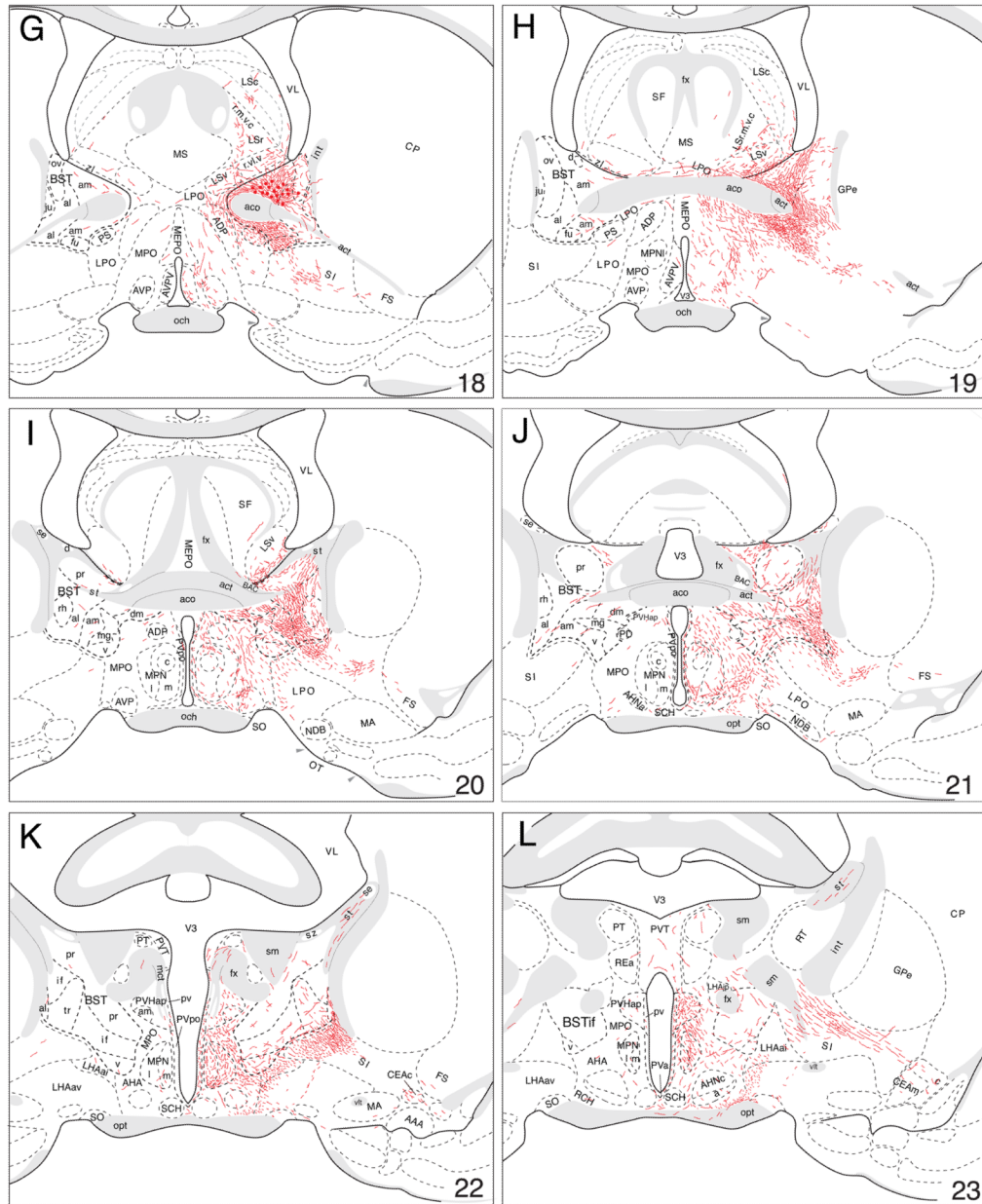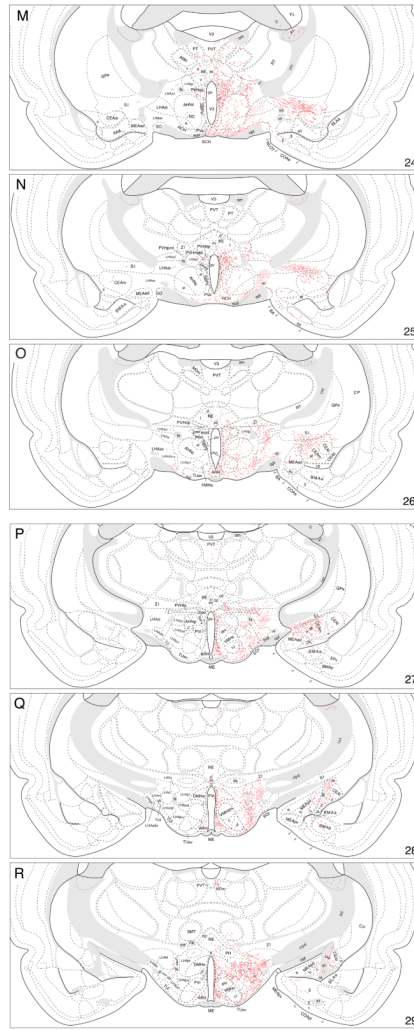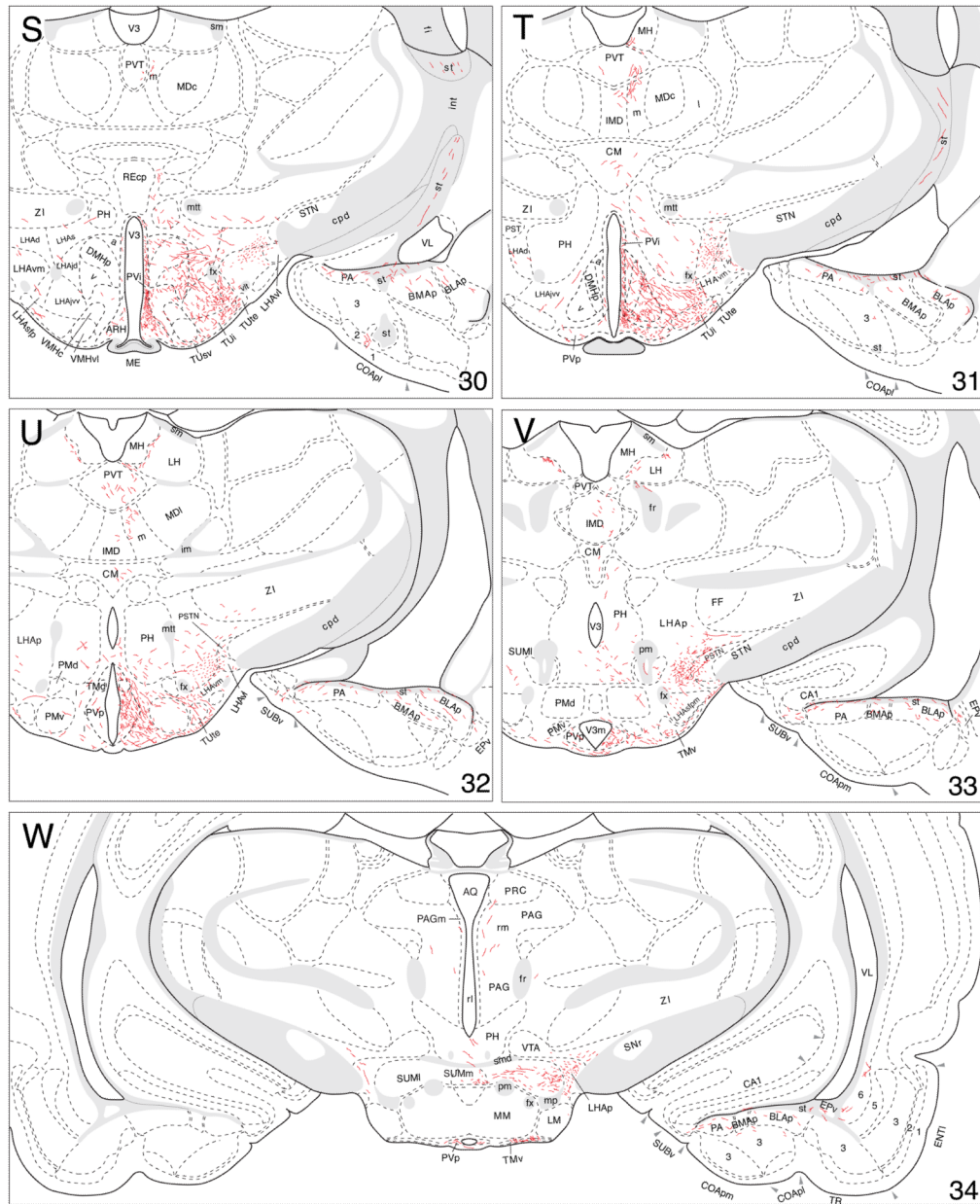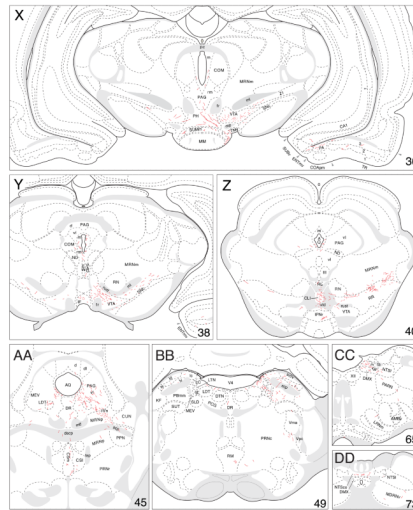
Fig. 9.
A summary of BSTam pathways and terminal fields. The distribution of PHAL-labeled axons (thin red lines) in experiment BST10 was plotted onto a series of standard or reference drawings of the rat brain derived from an atlas (Swanson, 2004), and arranged from rostral (A) to caudal (DD). The red dots in the dorsal BSTam at levels E–G indicate labeled neurons in the PHAL injection site (see Figs. 1–3). The key in the upper right corner of level A illustrates the meaning of terms used in the text to describe PHAL-labeled axons. Boutons-of-passage (bp) and terminal boutons (tb) are also referred to simply as terminals, whereas varicosities (v) may or may not form synapses (see Swanson, 2004). The scale of the drawings themselves is too small to illustrate these features. The number in the lower right corner of each drawing refers to the corresponding Atlas Level.
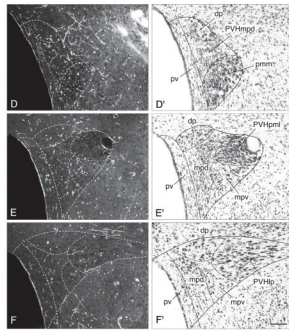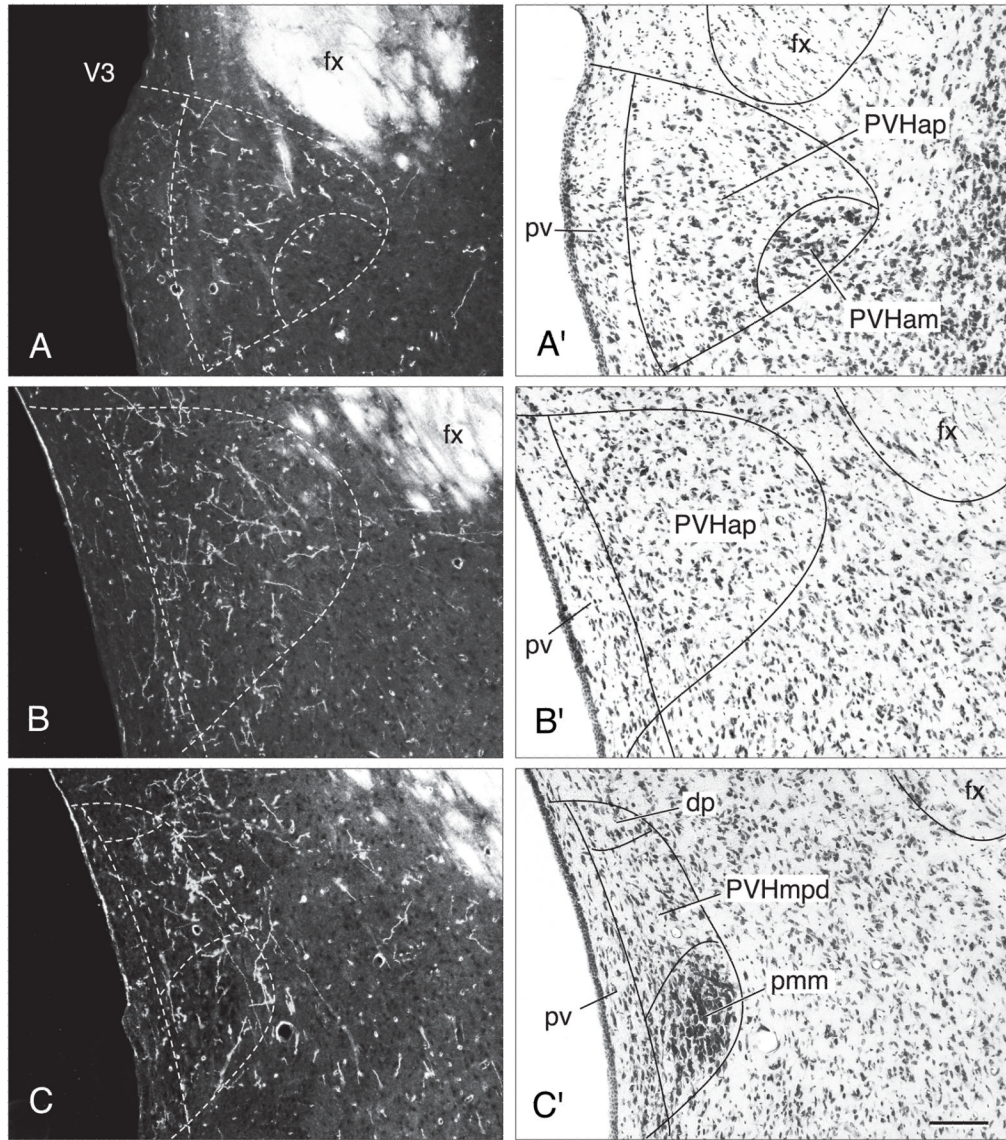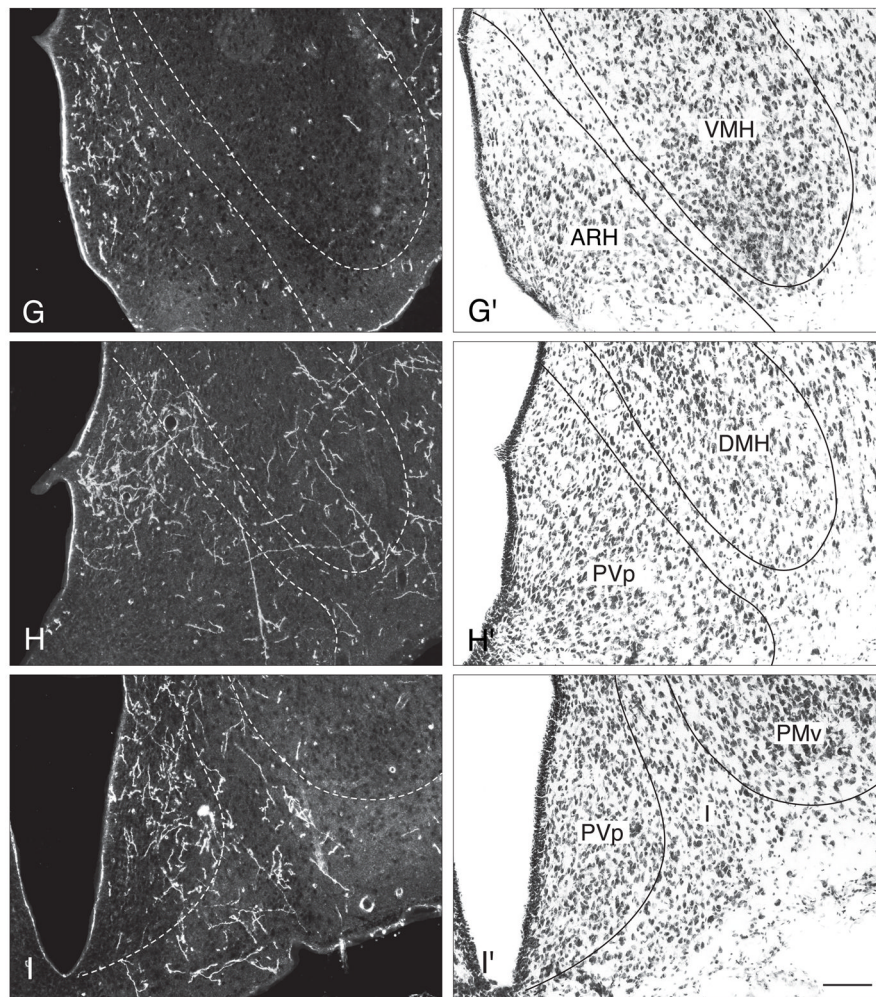
Fig. 10.
Darkfield photomicrographs showing the appearance of PHAL-labeled axons from the dorsal BSTam (experiment BST10; the one illustrated in Figure 9) in transverse histological sections through the hypothalamic paraventricular nucleus from rostral to caudal (A–F; about levels K–P in Fig. 9), arcuate nucleus (G: about level R in Fig. 9), and posterior periventricular nucleus (H,I; about levels T,U in Fig. 9). For subdivisions of the paraventricular nucleus, see the corresponding caudally adjacent thionin-stained transverse sections (A′–G′). Scale bar = 100 μm.
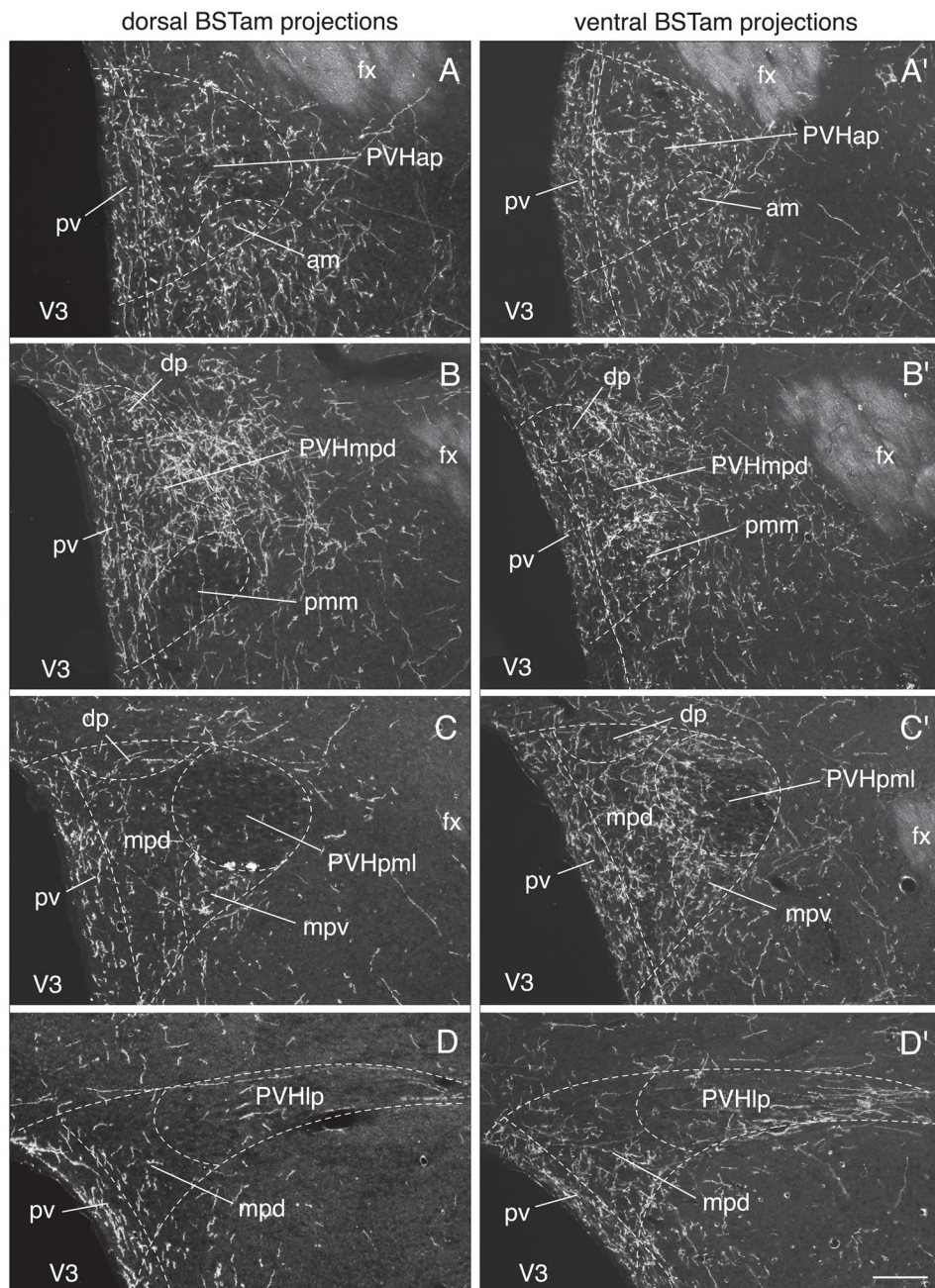
Fig. 11.
Photomicrographs (darkfield illumination) comparing the distribution of PHAL-labeled axons in four representative transverse levels through the hypothalamic paraventricular nucleus, arranged from rostral to caudal, from PHAL injections involving the dorsal BSTam (experiment BST25, A–D; with a larger injection site than BST10 illustrated in Fig. 10) or the ventral BSTam (experiment ACB12, A′–D′). In experiment ACB12, the PHAL injection site extends all the way to the rostral tip of the ventral BSTam. PHAL-labeled axons in experiment ACB12 display a similar distribution pattern to those labeled from other BSTam regions (e.g., in experiments BST25; and in experiment BST10, Fig. 10) in the periventricular part (A–D, A′–D′), anterior parvicellular and magnocellular parts (see A, A′),

and rostral regions of the dorsal parvicellular and dorsal zone of the medial parvicellular parts (see B,B′) of the paraventricular nucleus. However, in experiment ACB12 significantly more PHAL labeling is observed in the posterior magnocellular part (compare B and B′, C and C′) and caudal region of the dorsal zone of the medial parvicellular part (compare C and C′, D and D′). More PHAL labeling is also observed in the lateral parvicellular part in experimental ACB12 (compare D and D′). The approximate level of these photomicrographs is shown on levels K–P of Fig. 9. All scale bars = 100 μm.
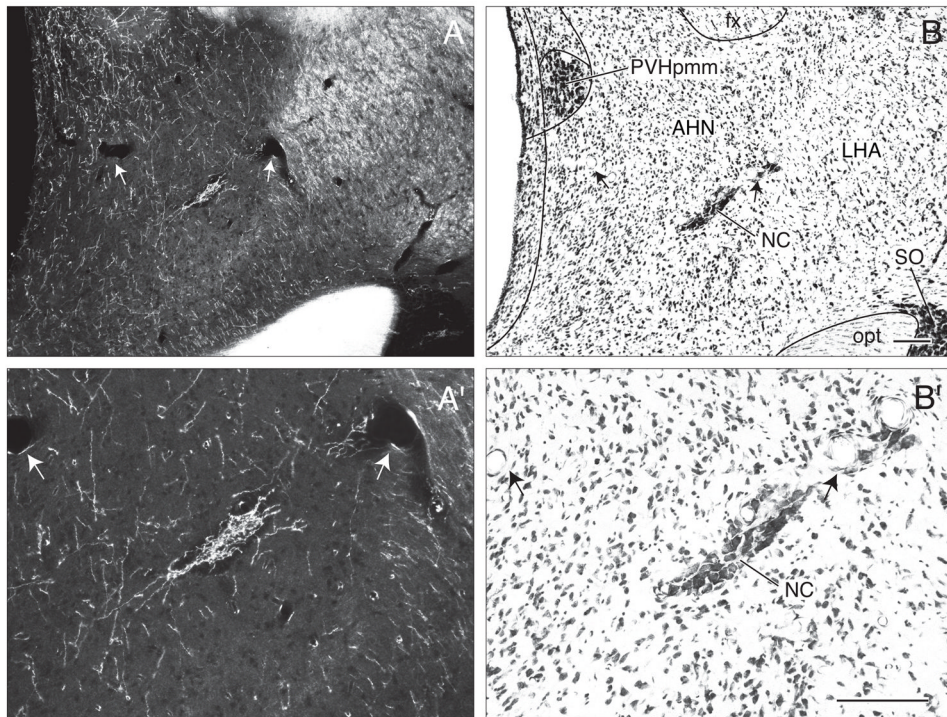
Fig. 12.
The darkfield photomicrographs on the left show at low (A) and higher magnification (A′) the distribution of PHAL-labeled axons in and around the anterior hypothalamic nucleus, and especially a dense terminal plexus in the nucleus circularis, from experiment ACB12 (cut in the transverse plane). This PHAL injection site involves the largest extent of the ventral BSTam of any experiment in this study, and spreads from the rostral end of the ventral BSTam also to include a few labeled neurons in the parastrial nucleus and BST fusiform nucleus, neither of which are thought to project to the nucleus circularis. Other PHAL injections involving the ventral BSTam do not label neurons in its rostral tip. For cytoarchitectonic comparison an adjacent Nissl-stained section is shown to the right (B, B′). These photomicrographs are at about level M of Fig. 9. All scale bars = 100 μm. For orientation, arrows indicate the same two blood vessels in each of the photomicrographs.
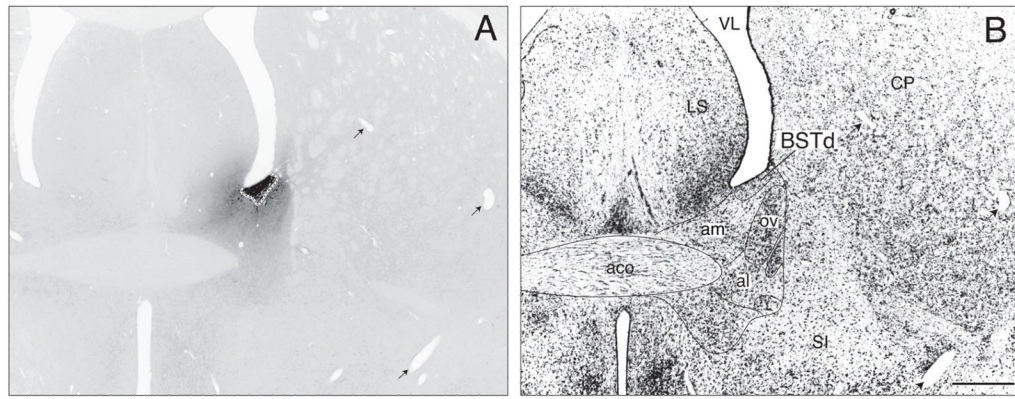
Fig. 13.
Brightfield photomicrographs to show the appearance of a PHAL injection site centered in the BST dorsal nucleus (A; experiment BST23), and an adjacent Nissl-stained section (B). Arrows in A and B indicate the same blood vessels. The region in (A) containing PHAL-labeled neuronal cell bodies (the effective injection site) is outlined with a dashed line. This injection site is also illustrated schematically in Figure 1, and its approximate location corresponds to Fig. 9I, where it can be seen that the BSTd is surrounded by the stria terminalis, which separates it clearly from the BSTam and BST oval nucleus. Scale bar = 500 μm.
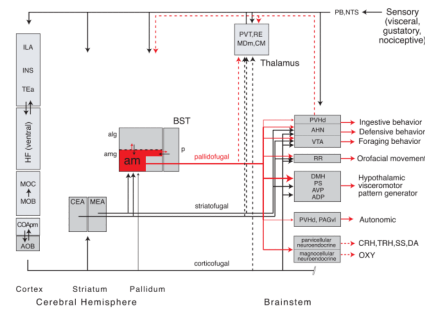
Fig. 14.
Schematic overview showing how the BSTam participates in a basic triple descending projection from the three major parts of the cerebral hemisphere to the brainstem motor system, with a thalamocortical feedback loop (dashed lines). Direct outputs of the BSTam itself are indicated in red. References for the circuitry are provided in the Discussion section, except as noted below. For clarity, details of ascending inputs to cerebral cortical areas, interconnections between cortical areas, and the descending targets of each indicated cortical area, are not illustrated (they are reviewed in Swanson, 2000; Dong et al., 2001a; Dong and Swanson, 2003). For the same reason, projections from the BSTam to other parts of the striatum (nucleus accumbens and lateral septal nucleus) and pallidum (substantia innominata), and to the behavioral state system (especially the supramammillary and tuberomammillary nuclei) also are not illustrated. Diagram adapted from Figure 32C in Swanson (2000).